FREEZE-THAW DURABILITY EVALUATION OF QUARRIED LIMESTONE COARSE AGGREGATES FOR TRANSPORTATION INFRASTRUCTURE APPLICATIONS

by

Benjamin M. Stark

A Thesis Submitted in

Partial Fulfillment of the

Requirements for the Degree of

Master of Science

in Engineering

at

The University of Wisconsin-Milwaukee

August 2022

ABSTRACT

EVALUATION OF DURABILITY OF EXISTING BASE AGGREGATES IN WISCONSIN PAVEMENTS

by

Benjamin M. Stark

The University of Wisconsin-Milwaukee, 2022
Under the Supervision of Professor Hani Titi

Aggregates are an important component of transportation infrastructure used as unbound base material and within Portland cement concrete (PCC) structures. In cold climate regions, seasonal freeze and thaw cycles cause damage to aggregate and impact pavements, bridges, and other transportation infrastructure performance. This research investigated Wisconsin quarried coarse aggregates for freeze-thaw durability as unbound aggregates as well as in PCC mixtures for pavement surface. A comprehensive laboratory testing program was conducted on 21 coarse aggregate samples consisting of calcareous and dolomitic limestone including sodium sulfate soundness, freeze-thaw testing, and absorption. Furthermore, three sources of these coarse aggregates were used to prepare concrete mixes, according to WisDOT mixture design for PCC pavements, and cast PCC cylinders for stiffness and strength evaluation due to rapid freeze-thaw conditioning. Results of the testing program demonstrated variable results for the investigated coarse aggregates in which poor correlation was exhibited between sodium sulfate soundness and freeze-thaw soundness testing on unbound aggregates. Variation in the mass loss values from freeze-thaw testing and sodium sulfate soundness testing for calcareous versus dolomitic limestone coarse aggregates suggests different mechanisms of aggregate degradation occur between the test methods. Testing on PCC cylinders with the

investigated coarse aggregates showed that the aggregate does not appear to have a significant impact on the rapid freeze-thaw degradation of concrete when a high-quality mixture and high entrained air content is utilized. Another reason could be that the applied number of freeze-thaw cycles did not result in a tangible aggregate damage within the PCC to significantly influence the PCC strength and stiffness.

TABLE OF CONTENTS

LIST OF FIGURES

LIST OF TABLES

ACKNOWLEDGEMENTS

I would like to give my deepest gratitude to Dr. Hani Titi for all your support, guidance, and help along the way. I would not have been able to complete this project without the substantial time and effort you spent on my behalf. I would also like to thank my Thesis Committee, Dr. Habib Tabatabai, Dr. Rani Elhajjar, and Dr. Ben Church, for their time and effort. In addition, I would like to thank Dr. Issam Qamhia for the significant assistance and input on this project.

I would also like to extend a special thanks to my coworkers in the Geotechnical Department at Giles Engineering Associates for their input, continual patience, and understanding.

Finally, thank you so much to my family for the constant support throughout my graduate career. I would not be where I am without their support and unsurmountable encouragement and reassurance.

Chapter 1

Introduction

Transportation infrastructure is an important economic asset for local, state, and federal governments, and is a costly investment to construct and maintain. It is critical that materials used in construction are durable to minimize infrastructure damage and maintain function throughout the planned economic lifecycle of the infrastructure asset. Natural aggregate is an important element in a pavement structure, as it is used as the base course layer and within the pavement structure (Portland cement concrete or hot mix asphalt surface layers). In cold climate regions, seasonal freeze and thaw cycles cause damage to aggregate and impact pavements, bridges, and other transportation infrastructure performance. Using quality aggregates that have relatively high freeze-thaw resistance reduces the likelihood of increased pavement damage, distress, degradation, and subsequently an increased pavement service life.

This research intends to evaluate the impact of freeze-thaw cycles, that typically occur in northern climates, on virgin Wisconsin quarried coarse aggregate performance. A good quality aggregate that performs well during freeze-thaw cycles will result in durable concrete and base materials. Such good performance can result in more economical design and estimation of the service life of pavements or other transportation infrastructure.

1.1 Objectives and Scope

The objectives of this research are to:

1) Investigate the durability of Wisconsin quarried coarse aggregates (crushed) for freeze-thaw resistance to degradation and breakage under freeze-thaw cycles using AASHTO T

103 and T 104, for freeze-thaw soundness and sodium sulfate soundness testing, respectively.

2) Evaluate the freeze-thaw performance using the conventional test method of manual cycles (chest freezer) versus using automated cycles (automated freezer system).
3) Investigate the impact of the coarse aggregate on the freeze-thaw performance of Portland cement concrete used in Wisconsin Department of Transportation (WisDOT) pavement construction.

This thesis studies coarse aggregates, as defined by the Wisconsin Department of Transportation (WisDOT, 2022), that are used in Portland cement concrete (PCC) pavement, bridge structures, and other transportation infrastructure. This study is limited only to coarse aggregates and Portland cement concrete used as pavement surface layer and does not include hot mix asphalt (HMA) surface layer as the HMA aggregate is coated with, and protected by, an asphalt binder, which significantly reduces water intrusion into coarse aggregates within HMA. Inclusion of a study of HMA aggregate would require a study of mix performance, which is outside the scope of this thesis. Additionally, this study is mainly limited to calcareous and dolomitic limestone coarse aggregates, as these types of aggregate are widely used in Wisconsin and are generally susceptible to freeze-thaw conditions.

1.2 Overview of Methodology

Performance evaluation of virgin Wisconsin coarse aggregates to freeze-thaw conditions was conducted using standard laboratory test methods and procedures. Samples of virgin coarse aggregate were collected from various quarries in Wisconsin by a WisDOT certified technician.

Then, aggregates were processed and subjected to an experimental testing program at the University of Wisconsin-Milwaukee Pavement Research Lab. Portland cement concrete mixtures were designed using WisDOT requirements for pavements in which the investigated coarse aggregates were used to cast 4-inch and 6-inch concrete cylinders for testing and evaluation. Laboratory testing was conducted on the PCC cylinders and on the coarse aggregate samples. Test results were collected from the conducted experiments and statistical analyses were performed.

Twenty-one coarse aggregate samples were studied: eight dolomitic and 13 calcareous limestone samples. Standard and modified laboratory tests were conducted on the coarse aggregate samples and concrete cylinders. Those tests are as follows: specific gravity and absorption were performed in accordance with AASHTO T 85 / ASMT C127 to determine the oven-dry specific gravity, saturated-surface-dry specific gravity, apparent specific gravity, and water absorption of the aggregates. Variations of the absorption test were also performed using vacuum saturation conditioning in accordance with the Manual for Michigan Test Methods MTM-113 (MDOT, 2020). The sodium sulfate soundness test was performed in accordance with AASHTO T 104 / ASTM C88 to measure the mass loss due to cyclic immersion and drying of coarse aggregate specimens in a sodium sulfate solution. Freeze-thaw soundness testing was performed in accordance with AASHTO T 103 to determine the mass loss of an aggregate specimen due to cyclic freezing and thawing. Freeze-thaw testing was performed with a set of duplicate samples on an automated freeze-thaw system and with a commercially available chest freezer for comparison.

Laboratory testing performed on the concrete cylinders included the following: rapid freeze-thaw testing in accordance with AASHTO T 161 / ASTM C666 with modifications to the

freeze-thaw cycle time and concrete specimen size. Measurement of the dynamic modulus of the concrete specimens was performed through the freeze-thaw testing with the fundamental resonant frequency impact method in accordance with ASTM C215. In addition, measurement of the ultrasonic pulse velocity of the samples was performed in accordance with ASTM C597 on saturated and oven dried cylinders to determine the dynamic modulus upon completion of the freeze-thaw cycles. Compressive strength testing in accordance with AASHTO T 22 / ASTM C39 was conducted on the cylinders after freeze-thaw testing and compared to control cylinders.

1.3 Organization of Thesis

This thesis is organized into five chapters. Chapter One includes the introduction, the objectives of the research, and scope of the project. Chapter Two contains a review of literature relating to the testing performed for the thesis and related studies, and an overview of the geology of Wisconsin. Chapter Three provides the methodology for the research. Chapter Four presents and discusses the results of testing program performed for the thesis. Finally, Chapter five presents a summary and conclusions of the research.

Chapter 2

Background

This chapter presents a review of relevant literature regarding the performance of coarse aggregates in terms of resistance to breakage and disintegration due to exposure to freeze-thaw cycles. Standard laboratory characterization tests performed on coarse aggregates and Portland cement concrete, including explanations and the significance of each test, are discussed first. An overview of the geologic history of Wisconsin is presented next, as relating to the coarse aggregates of sedimentary origin in Wisconsin, particularly calcareous limestone, and dolomitic limestone deposits. A literature review of relevant freeze-thaw durability testing procedures is also discussed in this chapter for unbound coarse aggregate particles and for aggregates in concrete specimens. Lastly, a review of the mechanisms leading to particle breakage/disintegration due to freezing and thawing is also discussed in this chapter.

2.1 Geologic Overview of Wisconsin Bedrock Sources

Wisconsin aggregates are quarried from bedrock or mined from sand and gravel pits. The bedrock geologic record of Wisconsin consists of two major time divisions: the Precambrian (Archean Eon and Proterozoic Eon) and the Phanerozoic Eon (WGNHS, 2005). Precambrian bedrock is older than 600 million years and primarily consists of igneous and metamorphic basement rock. The Phanerozoic is above the Precambrian and younger than 600 million years, and predominantly consists of sedimentary rocks and recent surficial glacial deposits (WGNHS, 2005). Precambrian rocks are present in the northern and northwestern regions of Wisconsin, whereas Phanerozoic bedrock is present in the southern, central, and western parts of the state.

The Precambrian bedrock of Wisconsin consists of Archean and Proterozoic Eons. Precambrian rocks are at relatively shallow depths or at the surface across a majority of Northern Wisconsin, and are overlain by several hundred feet of Paleozoic bedrock in South and Central Wisconsin (LaBerge, 1984). Archean-aged bedrock is older than 2,500 million years and consists of gneiss in Central and Northern Wisconsin as well as granitic intrusions in volcanic rocks. Archean bedrock in Wisconsin has been highly deformed (WGNHS, 2005).

Proterozoic Eon bedrock consists of four major groups. The oldest rock consists of sedimentary slates, greywacke and iron formations, and volcanic and intrusive igneous rocks that are approximately 1,800 million to 2,000 million years old. The igneous and intrusive suites from this time are mostly basaltic pillow lavas with some rhyolitic deposits from 1,850 million years ago. These rocks were extensively deformed during the Penokean Orogeny (LaBerge, 1984). The "Penokean aged" granites formed during the orogeny can be readily observed where Wisconsin red granite has been quarried in the north-central regions of the state. Following the Penokean Orogeny, relatively thick deposits of sandstone were deposited, metamorphosed to quartzite, and folded between 1,400 and 1,750 million years ago. Remnants of the Proterozoic quartzite are present at the Baraboo Quartzite syncline in Columbia and Sauk Counties, outcrops of the Barron Quartzite in the Blue Hills in Barron and Rusk Counties, and outcrops of the Rib Mountain Quartzite in Marathon County (WGNHS, 2005). Middle Proterozoic bedrock consist of granites in northeastern Wisconsin from the Wolf River complex from 1,400 to 1,500 million years ago (WisDOT, 2017). The final major Precambrian event in Wisconsin was the Keweenawan, which is characterized by basaltic lava flows associated with the mid-continental rift that extended from Lake Superior to Kansas. Keweenawan-aged rocks are present in northwestern Wisconsin and are from about 1,100 to 1,200 million years ago (LaBerge, 1984). Keweenawan bedrock consists of

older basalt and gabbro associated with volcanic activity from the rift activity, and younger sandstone. Precambrian time in Wisconsin is characterized by cycles of volcanic activity, sedimentary deposition and subsequent metamorphism, and erosion.

The Phanerozoic Eon consists of three eras, the Paleozoic, the Mesozoic, and the Cenozoic Eras. The Paleozoic consists of sequences of sandstone, shale, calcareous limestone, and dolomitic limestone; the Mesozoic is only possibly represented by gravels as no Mesozoic bedrock is present in Wisconsin; and the Cenozoic by glacial deposits (WGNHS, 2005). Paleozoic aged bedrock is present in the southern half of the state. The focus of this study is primarily on Phanerozoic calcareous and dolomitic limestone beds.

The Paleozoic Era is marked by several sea level transgressions and regressions that covered Wisconsin. Beginning in the Cambrian (501 to 488 million years ago), near-shore sediments were deposited, leaving interbedded sandstone and shales. As shown on Figure 2.1, Cambrian aged deposits stretch across the northwest and central portions of the state. Cambrian aged rocks consist of the Elk Mound, Tunnel City and Trempealeau Groups, that mainly consist of sandstone with interbedded shales. However, some dolomitic and calcitic limestone beds are present in Cambrian aged rocks.

Sea level changes continued throughout the Ordovician Period (488 to 444 million years ago) continuing sedimentary deposition. Ordovician aged rocks consist of: the Prairie du Chien Group, consisting of Oneota and Shakopee limestones with some sandstones; the Ancel Group, which contains the Glenwood shale and St. Peter Sandstone; the Sinnipee group, which includes the Platteville Limestone (which has interbedded shales), the Decorah formation of shaley limestone, the Galena formation of dolomitic and calcareous limestone, and the Maquoketa shale (which separates the upper Ordovician from the lower Silurian). Ordovician aged formations arch

across the eastern and southern portions of Wisconsin and are quarried for dolomitic and calcareous limestone. Sea levels submerged Wisconsin at the end of the Ordovician into the Silurian, and relatively thick limestone (later altered to dolomite) was deposited (WGNHS, 2005). Silurian aged rock is present along the eastern edge of the state, as shown on Figure 2.1, along the "Silurian Ridge." Silurian dolomite is quarried extensively for use as road base and concrete aggregate in these regions and is generally thinly-bedded to massive with sub-vertical and sub-horizontal jointing where extensively exposed (USGS, 1978). The youngest bedrock deposits in Wisconsin are Devonian-aged dolomite and shale. However, Devonian-aged rock is only present along Lake Michigan in Ozaukee and northern Milwaukee Counties. Bedrock was uplifted during the end of the Paleozoic, which is apparent in the eastward dip of Ordovician and Silurian aged rocks.

Within the last million years, during the Pleistocene, Wisconsin underwent series of glaciations that deposited ridges and hills of sand and glacial till, and created lakes across the state, except in the southwest. Sand and gravel pits are mined from former glacial kames or outwash deposits across the formerly glaciated portions of Wisconsin (LaBerge, 1984).

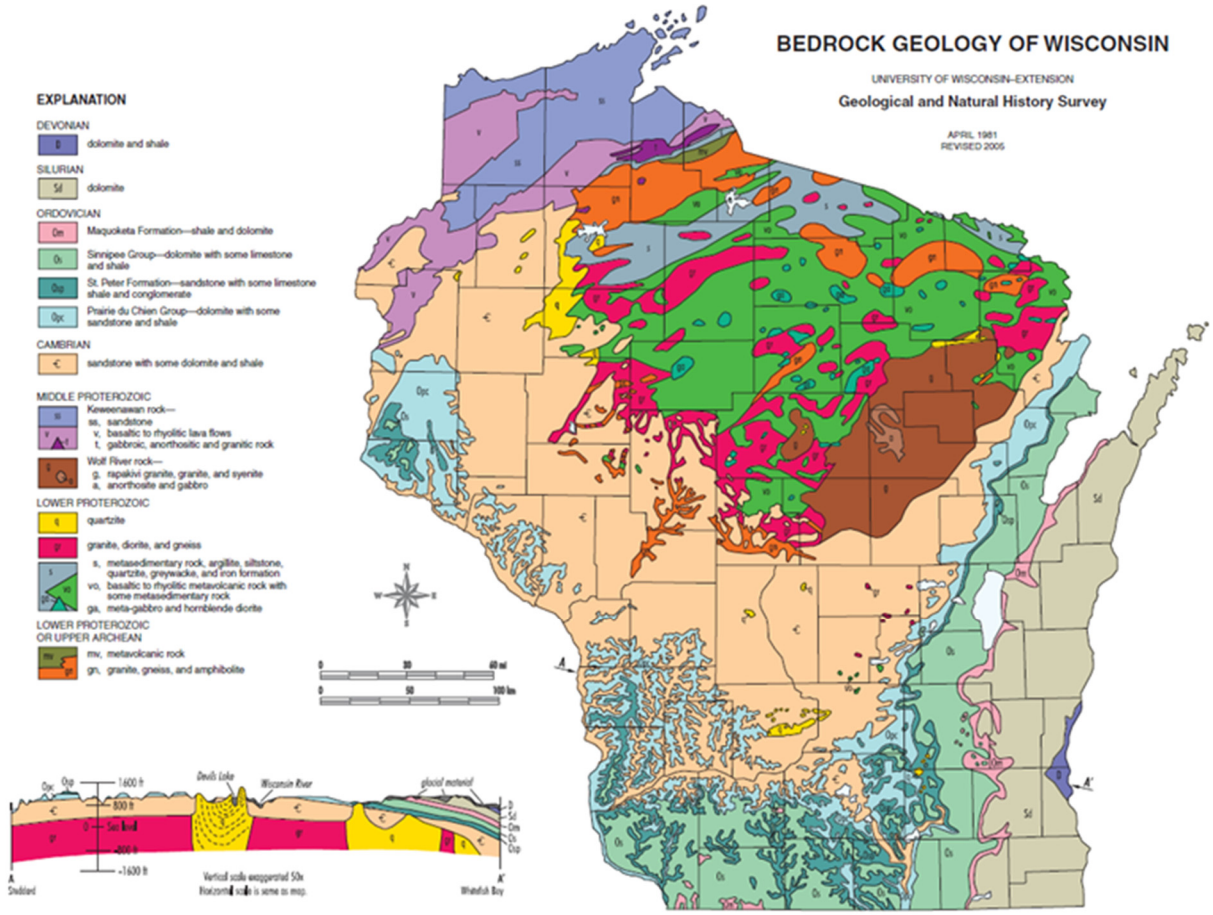

Figure 2.1: Bedrock geology map of Wisconsin (WGNHS, 2005)

2.2 Specific Gravity and Absorption of Coarse Aggregates

Specific gravity and absorption are physical properties of coarse aggregates that can assess aggregate quality. Specific gravity and absorption are determined from standard laboratory tests such as AASHTO T 85 *Standard Method of Test for Specific Gravity and Absorption of Coarse Aggregate* or ASTM C127 *Standard Test Method for Relative Density (Specific Gravity) and Absorption of Coarse Aggregate*. Specific gravity is the ratio of the mass of a given volume of aggregates to the mass of an equivalent volume of water. Absorption is the increase in mass of an aggregate due to water occupying the pores, excluding water adhering to

the exterior surface of the particle. Relatively high absorption values can indicate that an aggregate material is not durable (AASHTO, 2021). Pigeon and Pleau (1995) suggested that a limit of 2 percent absorption is used to avoid freeze-thaw damage of coarse aggregates (Pigeon and Pleau, 1995). The Minnesota Department of Transportation (MnDOT) Standard Specifications for Construction (MnDOT, 2020) requires that a Class B aggregate (quarried carbonates, rhyolites, schist) shall have a maximum absorption of 1.75% to be used for concrete pavement (Koubaa et al., 1997).

The Michigan Department of Transportation (MDOT) procedure for preparing coarse aggregate samples for freeze-thaw durability testing, as outlined in MTM-113 (MDOT, 2020), utilizes a vacuum saturation technique to maximize water absorption. The procedure requires samples to be oven-dried, placed under a vacuum of 28.5 inches of mercury for one hour, immersed in the chamber with water without breaking the vacuum, released from the vacuum, and then soaked for 23 hours. After the 24-hour vacuum saturation period, the samples are drained, and absorption testing is performed.

Stanton and Anderson (2009) evaluated the MDOT vacuum saturation procedure by studying the absorption using MTM-113 (MDOT, 2020) preparation. In this study, five coarse aggregates from US-23 Aggregate Test Road in Monroe County, Michigan, were sampled during construction. Four sources were geologically natural sources (gravel deposits and quarried carbonate rock), and one source was a blast furnace slag aggregate. The aggregates were dried and partitioned for various soaking periods. The aggregate soaking periods used were 1 day, 7 days, 30 days, 90 days, 180 days, 1 year, and 3 years. Additionally, five aggregate specimens from each source were vacuum saturated for comparison. The comparison of testing results for the various soaking times are shown in Figure 2.2.

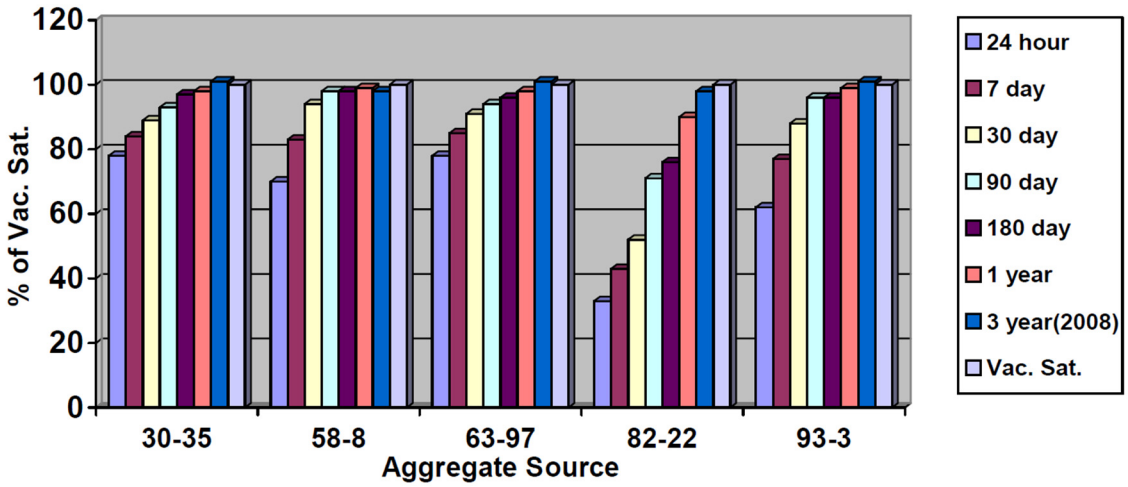

Figure 2.2: Results of absorption soaking times as a percent of vacuum saturation absorption for Michigan Aggregates (Stanton and Anderson, 2009)

Results of laboratory testing of Michigan aggregates indicated that the soaking period necessary to attain approximately 90 percent of vacuum saturation was 30 days for the geologically natural coarse aggregates. These aggregates reached vacuum saturation levels of absorption after one year of soaking. The comparison of absorption values using MTM 113 preparation procedure (vacuum absorption) and a standard 24-hour saturation per AASHTO T 85 (2021) indicated that the 24-hour saturation achieved 33 to 78 percent of the absorption measured using MTM-113 procedure (Stanton and Anderson., 2009). Thus, soaking time has an effect on the absorption of coarse aggregates.

Weyers et al. (2005) investigated testing methods for Wisconsin coarse aggregates. As part of their study, Wisconsin aggregate samples representing the full range of aggregates available in Wisconsin were tested for vacuum saturated specific gravity and absorption with a test method modified from ASTM C127. The aggregates were placed under a vacuum of 635 mm (25 inches) of mercury for 5 minutes and then saturated for 24 hours. Weyers et al. (2005) recommended the use of vacuum saturation over standard saturation of coarse aggregates to

evaluate absorption, since this procedure provided better representation of long-term field absorption of aggregates.

Another comparison between standard absorption and vacuum saturation absorption was performed by Richardson (2009) for the Missouri Department of Transportation (MoDOT). For this study, coarse aggregate samples were subjected to a vacuum of 27.5±2.5 mm (1.08±0.10 inches) absolute mercury pressure for 5 minutes. The vacuum chamber was then flooded, and the aggregates were submerged without breaking the vacuum for an additional 25 minutes. The material was then submerged at atmospheric pressure for 24 hours. Following saturation, AASHTO T 85 standard test procedure was followed. Evaluating coarse aggregate absorption following AASHTO T 85 standard was also performed on duplicate samples for comparison. Results of absorption testing are presented in Figure 2.3.

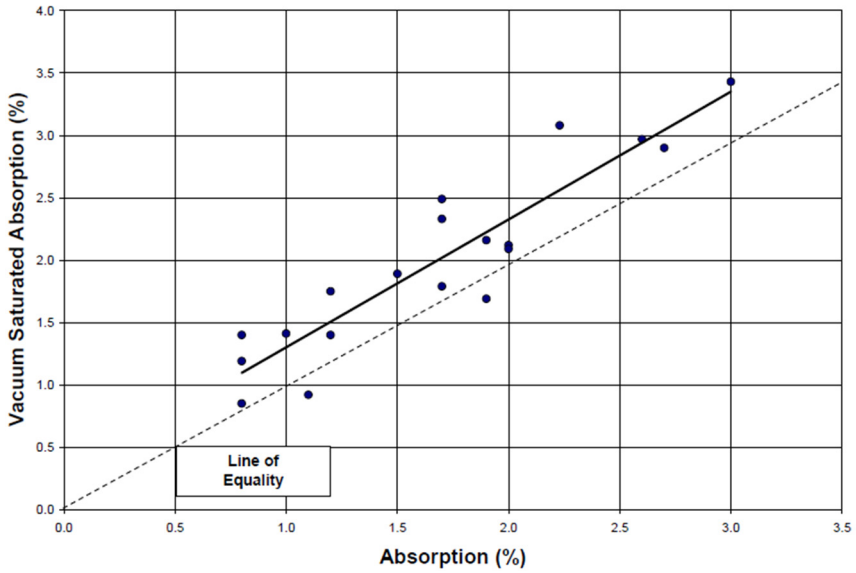

Figure 2.3: Comparison of vacuum saturated absorption (Missouri DOT modified conditioning) with AASHTO T 85 absorption conditioning (Richardson, 2009)

Richardson (2009) reported that the change in absorption using vacuum saturation condition ranged from (-0.2)% to +0.9% with an average increase of 0.3%. The comparison shown in

Figure 2.3 had an R value of 0.918. From these results, it is apparent that vacuum saturation conditioning affects the measured absorption values.

2.3 Laboratory Tests used as Aggregate Durability Indicators

The sodium sulfate soundness test is conducted to evaluate freeze-thaw resistance of aggregates by the mechanism of expansive force due to sodium sulfate or magnesium sulfate salt rehydration during the test (i.e., via wetting and drying cycles). AASHTO T 104 standard test procedure *Standard Method of Test for Soundness of Aggregate by Use of Sodium Sulfate or Magnesium Sulfate* (AASHTO, 2021) is comprised of five cycles. Each cycle consists of two phases: 1) immersing the aggregate specimen in the sodium sulfate or magnesium sulfate solution for 16 to 18 hours; 2) oven-drying the specimen to a constant mass. Rehydration and growth of the salt crystals within aggregate pores during immersion generates an internal expansive force that simulates the expansion of water during freezing conditions. Sieve analysis of the aggregate to determine mass loss is performed after completion of the five wetting/drying cycles. ASTM C88/C88M *Standard Test Method for Soundness of Aggregates by Use of Sodium Sulfate or Magnesium Sulfate* is another similar standard test used for the same purpose.

Sodium sulfate soundness is used by WisDOT as a main quality indicator of coarse aggregates for durable long-term performance. WisDOT requires that the maximum coarse aggregate mass loss using the sodium sulfate soundness test is 12% (WisDOT, 2022). The sodium sulfate soundness test is imprecise and has been shown to have relatively variable single operator coefficients of variation (Weyers et al., 2005). Williams and Cunningham (2012) evaluated the sodium sulfate soundness test method and found that the results variability decreased the reliability of the test.

Another direct freeze-thaw laboratory test is the AASHTO T 103 *Standard Method of Test for Soundness of Aggregates by Freezing and Thawing*. The procedure utilizes the mass loss of an unconfined aggregate after cyclic freezing and thawing. In this test, the aggregate is fractioned and placed in containers. Samples are conditioned via either procedure A: immersion in a 3 percent sodium chloride and water solution or 0.5 percent methyl alcohol and water solution and soaking the sample for 24±4 hours; or via procedure B: placing samples in a vacuum chamber and subjecting them to air pressure not exceeding 3.4 kPa (1.0 inch mercury), and then immersing the aggregate in an alcohol-water solution for 15 minutes; or procedure C, which is similar to procedure B but uses water instead of an alcohol-water solution. The purpose of the alcohol-water solution is to increase the penetration of water into aggregate pores during the soaking period (Qiao et. al, 2012). The samples are then placed into a container that contains ¼ inch of the alcohol-water solution, and spread into a layer that is one aggregate particle thick. The freeze-thaw cycles consist of cooling samples to -23±3ºC and holding for a minimum of 2 hours, and then thawing samples to 21±3ºC and holding for a minimum of 30 minutes.

AASHTO T 103 test procedure specifies 25 freeze-thaw cycles. However, some authorities can require 50, 16, and 25 cycles for sample preparation procedures A, B, and C, respectively (AASHTO, 2021). The WisDOT (2022) uses a modified version of the standard AASHTO T 103 in which the Methanol/water solution is used to prepare samples following procedure B and requires 16 freeze-thaw cycles be performed on coarse aggregates for durability evaluation. After the cycles are complete, samples are dried, sieved, and weighted to determine the weight loss.

AASHTO T 103 was evaluated by Williams and Cunningham (2012). As part of the study, triplicate samples of eight Arkansas limestone aggregate sources were prepared and tested

using procedure A of AASHTO T 103. A coefficient of variability of 36% was reported, and over half of the variability in the results was attributed to pure error related to the testing procedure. Pure error represents the variability of the test method and was quantified by removing the percentage of variability that could be attributed to differences between aggregate sources (Williams et al. 2012). Results of the variability analysis of the freeze-thaw test indicate that the test method is as variable as the tested aggregate sources.

2.4 Wisconsin Department of Transportation Coarse Aggregate Durability Testing

Tabatabai et al. (2013) investigated the performance of Wisconsin coarse aggregate for durability evaluation. Aggregate test results from WisDOT test database as well as data from tests performed on 69 aggregates by Weyers et al. (2005) were analyzed. A multi-parameter regression analysis was performed on the data from the WisDOT database. Results of the analysis are shown in Table 2.1 below. The intersection of each row and column indicates the correlation between the test results (Tabatabai et al., 2013).

Table 2.1: Results of multi-parameter regression analysis on Wisconsin aggregate test data; ABS=Absorption; LAA=Los Angeles Abrasion; SSS=Sodium sulfate soundness; UFT=Unconfined freeze-thaw (Tabatabai et al., 2013).

Variables	Micro-Deval	ABS	LAA	SSS	UFT
Micro-Deval	1	0.92709	0.75292	0.74870	0.39333
ABS	0.92709	1	0.75700	0.64853	0.33832
LAA	0.75292	0.75700	1	0.49310	0.32384
SSS	0.74870	0.64853	0.49310	1	0.12991
UFT	0.39333	0.33832	0.32384	0.12991	1

Results of the multi-parameter regression analysis indicated that the lowest correlation exists between the unconfined freeze-thaw test and other tests. Tabatabai et al. (2013) noted that the sodium sulfate soundness and unconfined freeze-thaw had the lowest correlation (R=0.13), even though the sodium sulfate soundness test has been regarded as a test to rapidly measure freeze-thaw resistance. Tabatabai et al. (2013) concluded that the unconfined freeze-thaw test is measuring an aggregate characteristic that is different from other tests and recommended the test to be a standalone requirement for any aggregate test protocol.

2.5 Iowa Pore Index Test (AASHTO TP 120)

Porosity, pore sizes, and pore size distribution are also important factors affecting the coarse aggregate durability and freeze-thaw performance. The Iowa Pore Index Test (Iowa DOT, 1980) also designated by AASHTO TP 120 *Standard Method of Test for Pore Index for Carbonate Coarse Aggregate* was developed to identify the potential of D-cracking within carbonate aggregates. For the test, samples of ½ inch and ¾ inch aggregates are placed under a pressure of 35 psi for 15 minutes (Iowa DOT, 1980). The volume of water entering the aggregate pores in the first minute is the primary load, and the volume entering the aggregate pores for the remaining 14 minutes is the pore index (secondary load). The primary load represents macropores and the secondary load represents micropores in the aggregate. The basis of the test is the assumption that micropores are directly related to the freeze-thaw durability of an aggregate (Bektas et al., 2016).

Bektas et al. (2016) conducted a study in which the Iowa Pore Index was compared to aggregate mass loss by unconfined freeze-thaw testing using ASTM C666 "*Standard Test Method for Resistance of Concrete to Rapid Freezing and Thawing*, soundness by sulfate

solution (ASTM C88), and Canadian unconfined freezing-thawing test (CSA A23.2-24A). Analysis of test results indicated that the mass loss of aggregates generally increases with the increase of the Iowa Pore Index; as depicted in Figures 2.4 (a) and (b).

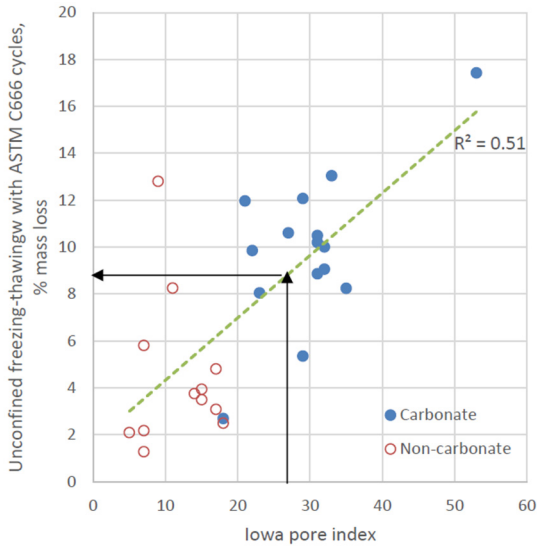

Figure 2.4 (a): Unconfined freezing-thawing test using ASTM C666 conditioning vs. Iowa pore index (Bektas et al., 2016)

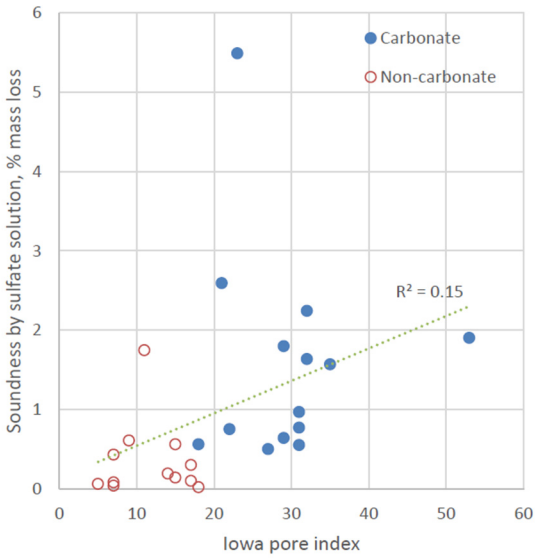

Figure 2.4 (b): ASTM C88 vs. Iowa pore index (Bektas et al., 2016)

2.6 Aggregate Breakage/Disintegration Mechanisms in Freezing Conditions

The pore structure of an aggregate plays an important role for long-term resistance of an aggregate to freeze-thaw conditions. Aggregate pore systems consist of pore space accessible from the surface and pore space isolated from the surrounding, which forms the majority of pores in an aggregate (Alexander and Mindess, 2005). The distribution of pores within an aggregate affects the saturation, and subsequently freeze-thaw durability. Porous material (aggregates) have a critical saturation where the material will only suffer from damage from freezing when the capillaries are saturated with greater than 91.7% of water (Powers, 1945). Critical saturation is typically about 91 percent for most aggregates. This typical value for critical saturation is

because water increases in volume by approximately 9 percent when it freezes and turns into ice. If the capillaries are saturated with more than 91 percent, the expansion resulting from ice formation will not be accommodated, and internal stresses will generate due to freezing (Alexander and Mindess, 2005).

Alexander and Mindess (2005) suggest that the main mechanism of freeze-thaw damage in an aggregate's pore structure is either because of the increase in volume of water during freezing or because of the pressure increase due to the growth of ice. Alexander and Mindess (2005) state aggregates can be classified into three groups in respect to freeze-thaw behavior: (1) aggregates having such a small pore volume (generally less than about 0.5 percent) that freezing expansion results in strains too small to cause cracking; (2) aggregates in which the hydraulic pressure generated by the flow of water ahead of a freezing front in a critically saturated pore system is able to crack the aggregate itself. Such aggregates must have a sufficiently low permeability and long enough flow path to generate high pressures; and (3) aggregates with a sufficiently high permeability to prevent hydraulic pressures being large enough to crack the aggregate. Smaller aggregates are considered less likely to suffer distress based on the suggested mechanism.

2.7 Resistance of Concrete to Rapid Freezing and Thawing (ASTM C666)

ASTM C666 standard test procedure evaluates the resistance of Portland cement concrete specimens to rapid cycles of freezing and thawing using either procedure A, rapid freezing and thawing of samples in water, or procedure B, rapid freezing of samples in air and thawing in water. A freeze-thaw cycle consists of lowering the temperature in the middle of the specimen from 4ºC to -18ºC (39.2ºF to -0.4ºF) and then raising it from -18ºC to 4ºC (-0.4ºF to 39.2ºF). The

free-thaw cycle is specified to be between 2 and 5 hours. ASTM specifies that the concrete test specimens shall be prism or cylinders made in accordance with ASTM C192/192M *Standard Practice for Making and Curing Concrete Test Specimens in the Laboratory* and Specification ASTM C490 *Standard Practice for Use of Apparatus for the Determination of Length Change of Hardened Cement Paste, Mortar, and Concrete*. During the test, samples are removed periodically (intervals not exceeding 36 cycles) to test resonant frequency for the relative dynamic modulus. The test is continued to 300 cycles or until a specimens' relative dynamic modulus of elasticity reaches 60% of the initial modulus, whichever occurs first (ASTM, 2021).

Crovetti and Kevern (2018) performed freeze-thaw durability tests in accordance with ASTM C666A for fully saturated rapid testing procedure. The freeze-thaw testing was performed on concrete prisms that were 3 in. by 4 in. by 12 in. The prisms were saw-cut from pavement test strips with two mix designs: one using southern Wisconsin limestone aggregates, and the other using northern Wisconsin igneous gravel aggregates. During the testing, the dynamic modulus and mass of the concrete prisms were measured every 30 freeze-thaw cycles. Freeze-thaw testing on specimens from each concrete mix was performed to 300 cycles, and to 600 cycles for select specimens. Test results of the measured dynamic modulus normalized relative to the initial dynamic modulus before specimen conditioning for the specimens made with limestone (relative dynamic modulus) with number of cycles are shown below in Figures 2.5 (a) and (b).

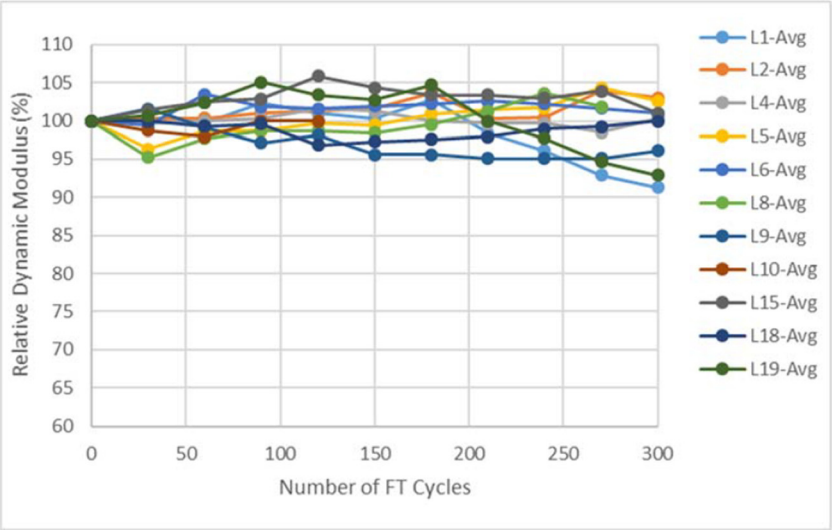

Figure 2.5 (a): Limestone freeze-thaw results after 300 cycles (Crovetti and Kevern, 2018).

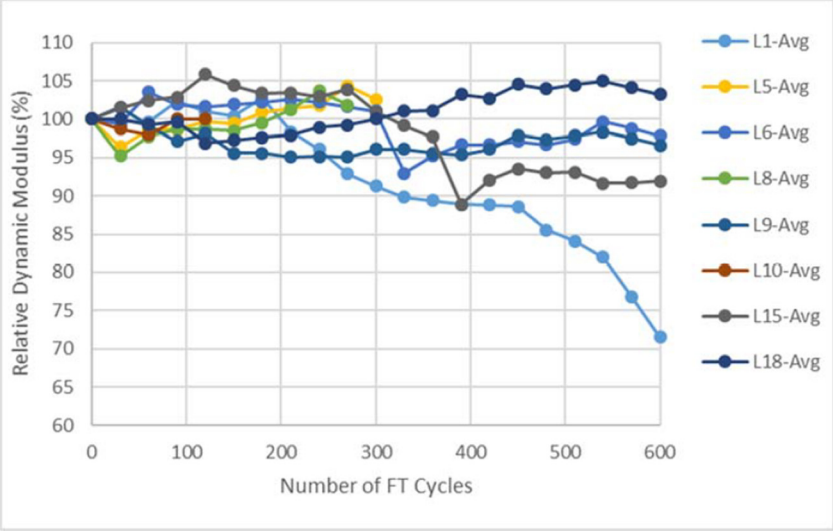

Figure 2.5 (b): Limestone freeze-thaw results after 600 cycles (Crovetti and Kevern, 2018)

Crovetti and Kevern (2018) reported that the concrete specimens made with limestone aggregates and granite gravel maintained high durability levels after 600 cycles. Only one concrete specimen made with limestone (specimen L01) exhibited a low relative dynamic modulus that decreased below 90% after about 330 through 600 freeze-thaw cycles, decreasing below 75 percent at cycle 600.

Hamoush et al. (2011) studied the freeze-thaw durability of high strength concrete prisms (3 in. by 4 in. by 16 in.). For the study, ASTM C666 procedures were followed for freeze-thaw

conditioning and the dynamic modulus was measured before starting freeze-thaw cycles, at 40 cycles, at 70 cycles, and at 100 cycles. Hamoush et al. (2011) reported that the measured dynamic modulus increased from 0 to 40 cycles and then decreased from 40 to 100 cycles (Hamoush et al., 2011). Results of the longitudinal and transverse modulus measurements are shown on Figures 2.6 (a) and (b).

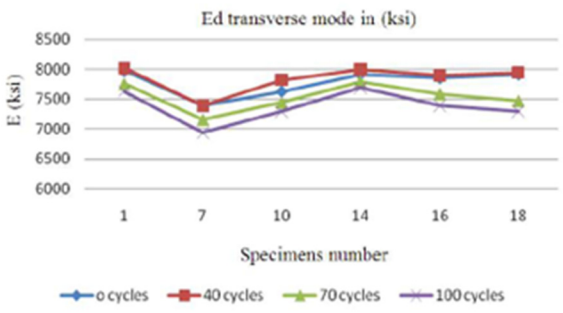

Figure 2.6 (a): Transverse dynamic modulus of concrete samples with respect to freeze-thaw cycles (Hamoush et al. 2011)

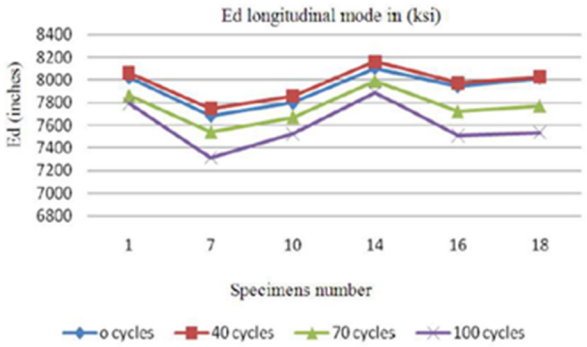

Figure 2.6 (b): Longitudinal dynamic modulus of concrete samples with respect to freeze-thaw cycles (Hamoush et al. 2011)

A study conducted by Chen and Qiao (2014) measured the dynamic modulus of concrete prisms (3 in. by 4 in. by 16 in.). Samples were freeze-thaw conditioned in accordance with ASTM C666 procedure A. The mix design was kept constant for all the concrete specimens, and the dynamic modulus of the prims were measured. Chen and Qiao (2014) reported that the larger variance of dynamic modulus between specimens was more apparent after 600 freeze-thaw cycles. Additionally, all the samples relative dynamic modulus values had dropped below 60% for all samples after 1,200 freeze-thaw cycles, which is considered the failing threshold (Chen and Qiao, 2014). The results of the study are shown in Figures 2.7 (a) and (b).

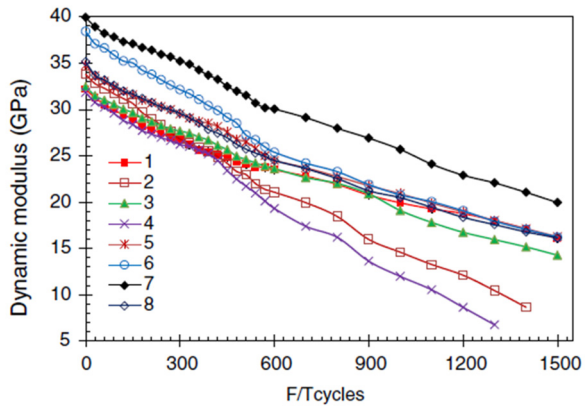

Figure 2.7 (a): Dynamic modulus of concrete samples with respect to freeze-thaw cycles (Chen and Qiao, 2014)

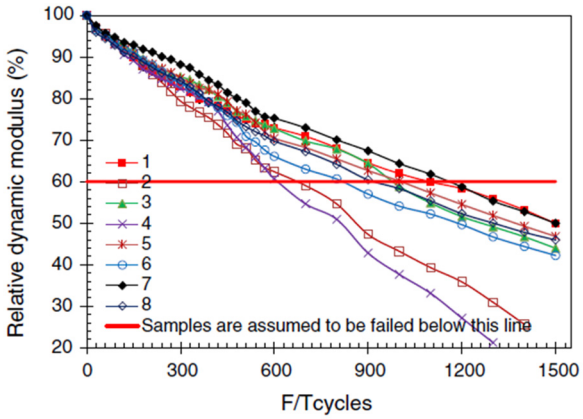

Figure 2.7 (b): Relative dynamic modulus of concrete samples with respect to freeze-thaw cycles (Chen and Qiao, 2014)

The effect of rapid freeze-thaw cycles on concrete durability, beyond 300 cycles, was studied by Olba et al. (2016) using ASTM C666 procedure A. In the study, Olba et al. (2016) measured the mass loss and dynamic modulus of concrete beam specimens (3 in. by 4 in. by 15.5 in.) throughout the test, to 3,200 freeze-thaw cycles. After 3,200 freeze-thaw cycles, a majority of the tested samples showed an excellent freeze-thaw performance and possessed relative dynamic modulus values above 80%. Additionally, the relationship between freeze-thaw cycles and sample degree of saturation was studied using sealed concrete samples with various degrees of saturation. Olba et al. (2016) concluded that there is a critical degree of saturation that the concrete must possess in order for freeze-thaw related failure to occur. Results of the freeze-thaw testing on the investigated concrete specimens indicated that the critical degree of saturation is around 88% (Olba et al., 2016).

2.8 Fundamental Resonant Frequencies of Concrete (ASTM C215)

The fundamental resonant frequency test procedure is provided in ASTM C215 *Standard Test Method for Fundamental Transverse, Longitudinal, and Torsional Resonant Frequencies of*

Concrete Specimens (ASTM, 2021). ASTM C215 test procedure provides two methods for measurement: (1) the use of a driving circuit with a variable frequency oscillator and a pickup circuit to measure the frequency through the specimen; and (2) impacting the specimen with 110 gram steel ball peen hammer and measuring the frequency with an accelerometer connected to a frequency analyzer. The dynamic Young's modulus of elasticity can be calculated using the fundamental frequencies measured (ASTM, 2021). The dynamic modulus for the transverse frequency was calculated using equation 1 (shown below) in ASTM C 215 (2020):

$$Dynamic\ E = CMn^2 \qquad \text{(Equation 2.1)}$$

Where:

M = mass of specimen, kg
n = fundamental transverse frequency, Hz
C = 1.6067 (L^3T/d^4), m^{-1} for a cylinder
L = length of specimen, m
d = diameter of cylinder, m
T = correction factor depending on radius of gyration K ($d/4$ for a cylinder) to the length of the specimen, L, and on Poisson's ratio

The dynamic modulus for the longitudinal frequency is calculated using equation 2 (shown below) in ASTM C 215 (2020):

$$Dynamic\ E = DM(n')^2 \qquad \text{(Equation 2.2)}$$

Where:

n' = fundamental longitudinal frequency, Hz
D = 5.093 (L/d^2), m^{-1} for a cylinder

2.9 Pulse Velocity Through Concrete (ASTM C597-16)

The pulse velocity procedure through concrete is provided in ASTM C597 *Standard Test Method for Pulse Velocity Through Concrete* (ASTM, 2021). The standard test procedure

measures the propagation velocity of longitudinal stress wave pulses (P-waves) through a concrete specimen. Longitudinal stress waves must have a resonant frequency in the range of 20 to 100 kHz and are generated from an ultrasonic pulse generator. A receiving circuit measures the travel time through the concrete specimen, which is used to calculate the dynamic modulus of elasticity of the concrete specimen (ASTM, 2021).

The propagated P-wave velocity is a factor of the properties of the transport medium and is affected by Young's Modulus, Poisson's Ratio, and material density. In general, materials with higher densities have relatively higher P-wave velocities (Dashti, 2016). Typical P-wave velocities through concrete are reported to be between 3000 m/s and 5000 m/s (Trifone, 2017).

The Dynamic Modulus of Elasticity for a concrete cylinder is calculated using the cylinder dimensions, and weight using equation 3 (shown below) in ASTM C 597 (2016):

$$V = \sqrt{\frac{E(1-\mu)}{\rho(1+\mu)(1-2\mu)}} \qquad \text{(Equation 2.3)}$$

Where:

V = ultrasonic pulse velocity
E = dynamic modulus of elasticity
μ = dynamic Poisson's ratio
ρ = specimen density

Several factors may affect the measurement of the ultrasonic pulse velocity through concrete. Temperature and concrete sample moisture can both affect the velocity. However, variations in the concrete temperature between 10ºC and 30ºC have shown to cause no significant change in pulse velocity (IAEA, 2002). Additionally, free water in the voids of concrete can also affect the measured pulse velocity. Candelaria et al. (2020) demonstrated a positive correlation between P-wave velocities and concrete saturation. Relatively higher concrete saturation values result in higher measured pulse velocities.

2.10 Relationship Between the Resonant Frequency and UPV Testing

Both the pulse velocity test (ASTM C597) and the impact resonant frequency test (ASTM C215) allow for the evaluation of the dynamic elastic modulus of a concrete specimen. Trifone (2017) determined the dynamic elastic modulus using both the ultrasonic pulse method and the resonant frequency method on 4 in. by 8 in. concrete cylinders, 6 in. by 12 in. concrete cylinders, and 3 in. by 4 in. by 16 in. concrete prisms. Test results indicated that the dynamic elastic modulus calculated from an ultrasonic pulse test is 10% higher than the dynamic modulus determined through resonant frequency impact testing. Additionally, a coefficient of determination, R^2=0.97, was reported between the ultrasonic pulse velocity dynamic modulus and the resonance impact dynamic modulus (Trifone, 2017)

2.11 Compressive Strength of Cylindrical Concrete Specimens (ASTM C39)

ASTM C39 *Standard Test Method for Compressive Strength of Cylindrical Concrete Specimens* procedures measure the compressive strength of cylindrical concrete specimens. Concrete specimens may consist of molded concrete cylinders or concrete cores. A compressive axial load of 0.25±0.05 MPa/s is applied continuously to the cylinder until the cylinder fails or "breaks." The compressive strength of the cylinder is calculated by diving the maximum load reached by the cross-sectional area of the cylinder. The compressive strength is a parameter used for concrete quality (ASTM, 2021).

Chapter 3

Research Methodology

In this chapter, the research methods and test procedures performed in this study to investigate the freeze-thaw durability of coarse aggregates are described in detail. The research methodology includes descriptions of the selected coarse aggregate samples, and sample preparation and testing for both unbound coarse aggregate and the PCC (which contained the subject aggregates).

3.1 Investigated Coarse Aggregates

Coarse aggregates selected for this research were part of a larger study by Titi et al. (2022), currently underway at the University of Wisconsin-Milwaukee (UWM). Calcareous and dolomitic limestone crushed coarse aggregate samples, of sedimentary rock origin, were obtained from various quarries located in the southern, southeastern, southwestern, and northeastern regions of Wisconsin. The sampling was conducted by WisDOT certified technicians to ensure that representative coarse aggregate samples were properly collected and processed for the laboratory testing program. These aggregates consist of crushed stone particles obtained from quarries. The size fraction of the collected aggregates consisted of 1¼ in. aggregate base, concrete #1, and concrete #2 sizes as described by WisDOT Standard Specifications for Highway and Structure Construction (WisDOT 2022). Five-gallon buckets of each coarse aggregate type were collected and transported to the UWM Geotechnical and Pavement Research Laboratory for processing and testing. For this study, a total of 13 calcareous

and 8 dolomitic limestone coarse aggregate sources were collected. Figure 3.1 depicts some of the collected aggregates.

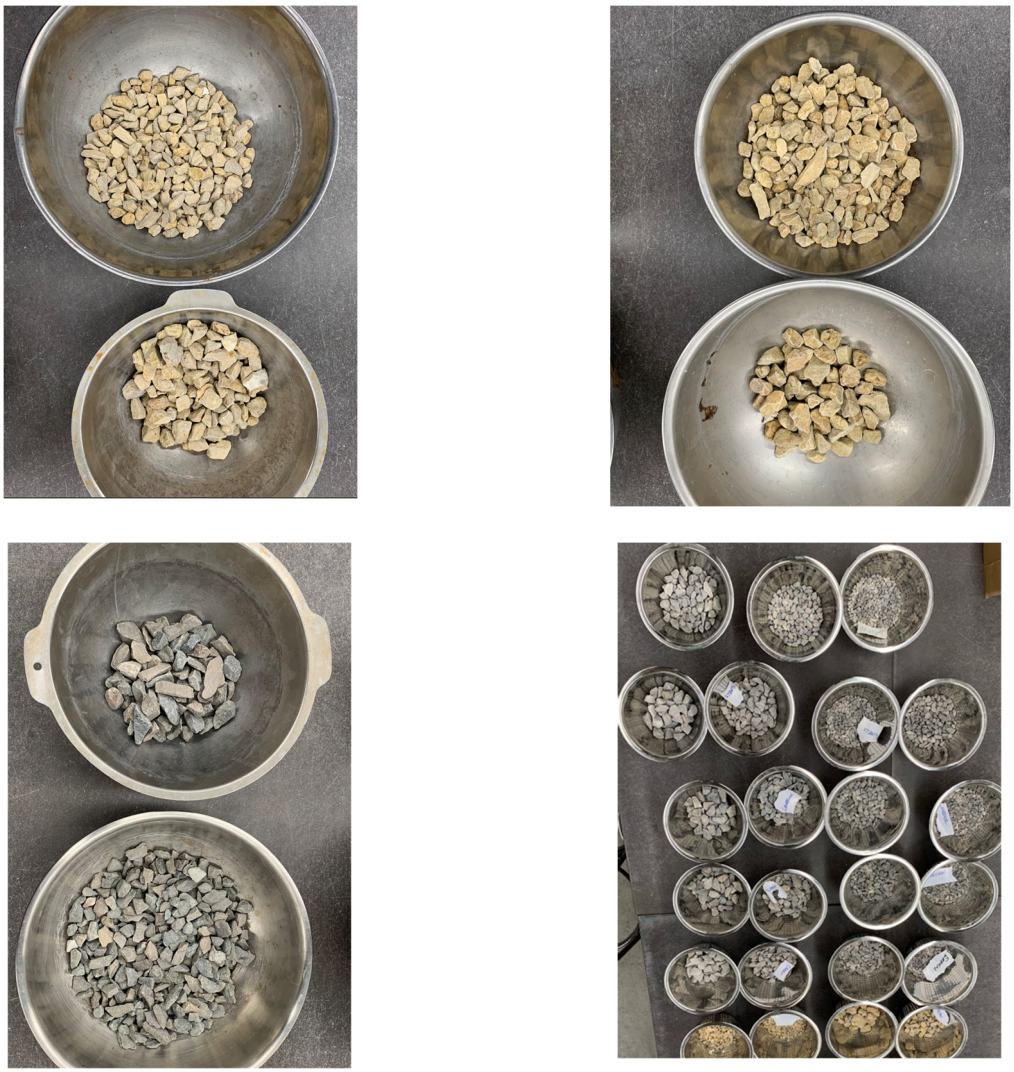

Figure 3.1: Pictures of typical calcareous and dolomitic limestone coarse aggregates used for this study

The coarse aggregates collected were subjected to standard test procedures, as presented in Table 3.1, to evaluate their specific gravity, absorption, sodium sulfate soundness, and freeze-thaw soundness. In addition, Table 3.2 presents the laboratory test matrix on the investigated coarse aggregate specimens.

Table 3.1: Laboratory tests conducted on aggregate samples and concrete specimens

Standard Test Procedure	Standard Designation	
	ASTM	AASHTO
Standard Test Method for Relative Density (Specific Gravity) and Absorption of Coarse Aggregate (ASTM) Standard Method of Test for Specific Gravity and Absorption of Coarse Aggregate (AASHTO)	C127-15	T 85-21
Standard Test Method for Soundness of Aggregates by Use of Sodium Sulfate or Magnesium Sulfate	C88-13	T 104-99
Standard Test Method for Soundness of Aggregates by Freezing and Thawing	-	T 103-08
Vacuum Absorption Test (Modified)	MDOT MTM 113	
Standard Test Method for Resistance of Concrete to Rapid Freezing and Thawing	C666-97	T 161-21
Standard Test Method for Air Content of Freshly Mixed Concrete by the Pressure Method	C231-09a	T 152-20
Standard Test Method for Resistance of Concrete to Rapid Freezing and Thawing (Modified)	C666/C666M-15	T 161-21
Standard Test Method for Fundamental Transverse, Longitudinal, and Torsional Resonant Frequencies of Concrete Specimens	C215-19	-
Standard Test Method for Pulse Velocity Through Concrete	C597-16	-
Standard Test Method for Compressive Strength of Cylindrical Concrete Specimens	ASTM C39/C39M-21	T 22M/T 22
Standard Test Method for Static Modulus of Elasticity and Poisson's Ratio of Concrete in Compression	C469/C469M-14e1	-

3.1.1 Specific Gravity and Absorption

The coarse aggregate samples collected were processed in accordance with AASHTO T 85 standard test procedure in which the bulk specific gravity G_s (oven dry), saturated surface dry specific gravity G_s (SSD) and apparent specific gravity G_s (Apparent) were calculated from test measurements. Moreover, the absorption was calculated from the AASHTO T 85 test measurements. The test equipment at UWM Geotechnical and Pavement Research Laboratory used in this study conform to the standard test procedure requirements, and are periodically calibrated.

Table 3.2: Laboratory tests conducted on aggregate samples

Geologic Description	Sample I.D.	Specific Gravity (AASHTO T85)	Absorption (AASHTO T85)	Vacuum Absorption (AASHTO T85) (MTM-113 Conditioning)	Sodium Sulfate Soundness (AASHTO T104)	Freeze-Thaw Testing with Automated Freezer (AASHTO T104)	Freeze-Thaw Testing with Chest Freezer (AASHTO T104)
Calcareous Limestone	CLS-Q-1	✓	✓	✓	✓	✓	✓
	CLS-Q-2	✓	✓	✓	✓	✓	
	CLS-Q-3	✓	✓	✓	✓	✓	
	CLS-Q-4	✓	✓	✓	✓	✓	✓
	CLS-Q-5	✓	✓	✓	✓	✓	
	CLS-Q-6	✓	✓	✓	✓	✓	
	CLS-Q-7	✓	✓	✓	✓	✓	
	CLS-Q-8	✓	✓	✓	✓	✓	✓
	CLS-Q-9	✓	✓	✓	✓	✓	
	CLS-Q-10	✓	✓	✓	✓	✓	
	CLS-Q-11	✓	✓	✓	✓	✓	
	CLS-Q-12	✓	✓	✓	✓	✓	✓
	CLS-Q-13	✓	✓	✓	✓	✓	
Dolomitic Limestone	DLS-Q-1	✓	✓	✓	✓	✓	✓
	DLS-Q-2	✓	✓	✓	✓	✓	✓
	DLS-Q-3	✓	✓	✓	✓	✓	
	DLS-Q-4	✓	✓	✓	✓	✓	✓
	DLS-Q-5	✓	✓	✓	✓	✓	✓
	DLS-Q-6	✓	✓	✓	✓	✓	
	DLS-Q-7	✓	✓	✓	✓	✓	✓
	DLS-Q-8	✓	✓	✓	✓	✓	

3.1.2 Vacuum Absorption Test

Vacuum absorption tests were performed on the investigated coarse aggregate samples in accordance with the test procedure described in MTM 113 (MDOT, 2020). This procedure was discussed in Chapter 2 of this Thesis. Pictures of the test setup are shown in Figure 3.2.

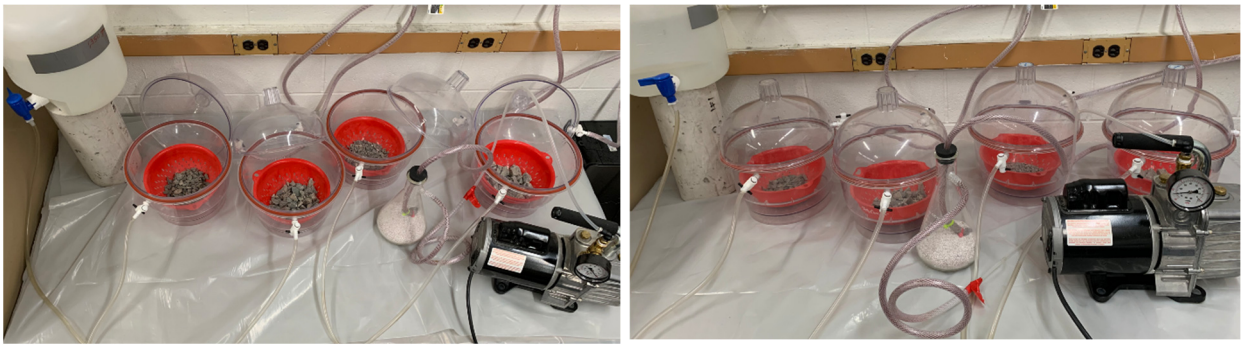

Figure 3.2: Vacuum desiccator and immersion system setup

3.1.3 Sodium Sulfate Soundness Test

The sodium sulfate soundness test was performed on the coarse aggregate samples in accordance with AASHTO T 104 standard test procedure. Sodium sulfate solution was prepared to the standard concentration range and was verified by the required specific gravity range. Sieve analysis was used to separate samples into the size fractions per AASHTO T 104 requirements (i.e., passing 1½″ and retained on 1″, passing 1″ and retained on ¾″, passing ¾″ and retained on ½″, passing ½″ and retained on $^{3}/_{8}$ ″, and passing $^{3}/_{8}$ ″ and retained on #4 sieve). The coarse aggregate size fractions were washed, dried, weighed to the required weight (specimens), placed in a stainless steel colander, and then immersed in sodium sulfate solution inside a container placed in a temperature-controlled water tank for 18 hours (wetting cycle), as depicted in Figure 3.3. The coarse aggregate specimens were then removed from the sodium sulfate solution, drained, then place in the oven for the drying cycle. During the drying cycle, the specimens were

kept in the same stainless-steel colander during the wetting/drying cycles to avoid aggregate particles disturbance during the test. At the end of the fifth wetting/drying cycle, the coarse aggregate specimens, while still in the same colander were stacked without contact by using plastic colanders for separation. Then, the colanders were placed in a system in which they were washed by flooding from the bottom of the wash tub until sodium sulfate was completely removed, which was verified by testing with a Barium Chloride solution. Finally, the aggregate fractions were dried after the washing process, sieved using the appropriate sieve size for each fraction, and then weighed so that the mass loss due to five cycles of sodium sulfate wetting/drying could be calculated.

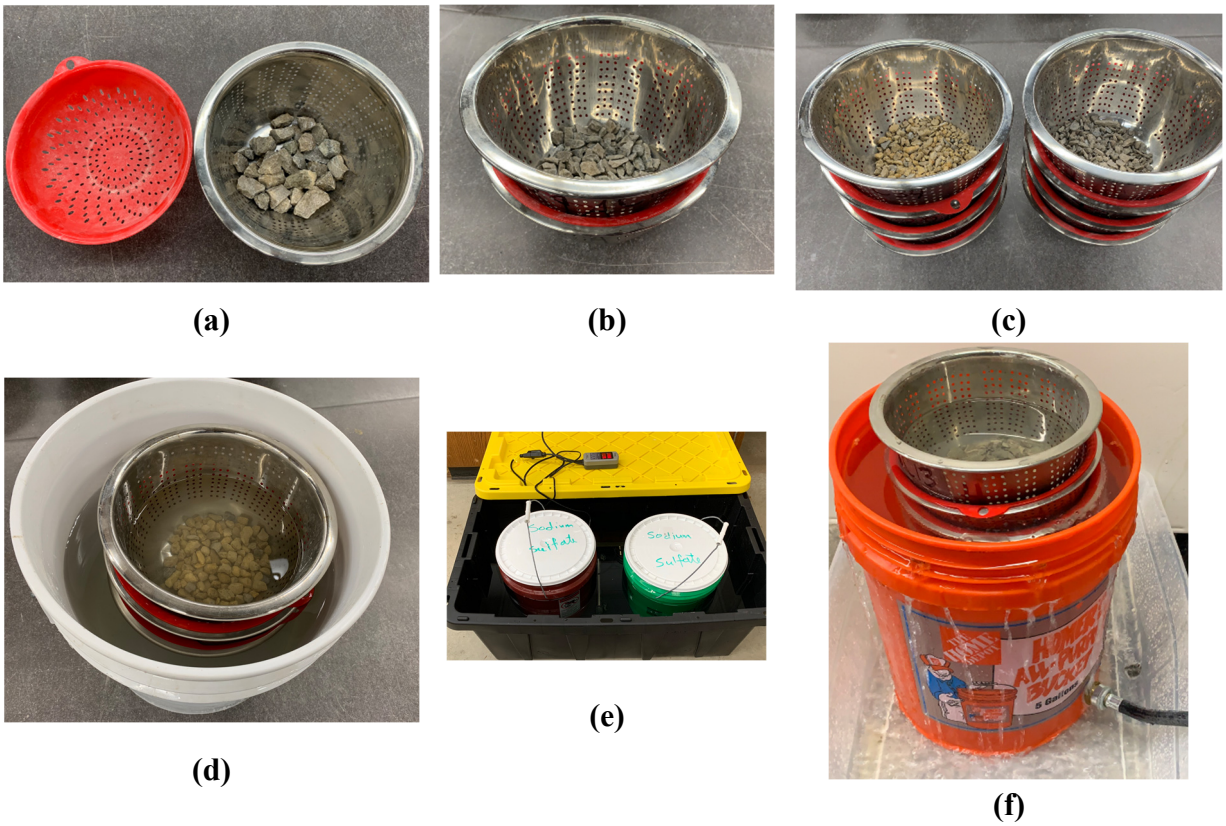

Figure 3.3: (a) Colanders used to hold coarse aggregates; (b) Typical colander stacking practice; (c) Example of colander stacks for SSS test containing calcareous limestone (left) and dolomitic limestone (right) aggregate specimens; (d) Colander stack in Sodium Sulfate solution bucket; (e) Sodium Sulfate solution buckets in temperature regulated water bath; (f) Setup for flooding colander stacks to wash specimens

3.1.4 Soundness of Aggregates by Freezing and Thawing

The investigated coarse aggregates were subjected to the standard soundness test procedure following AASHT T 103. Specimens of coarse aggregate size fractions were prepared per AASTHO T 103 requirements (the same procedure used to prepare specimens for AASHTO T 104). In this study, AASHTO T 103 procedure B was used to prepare the coarse aggregate specimens and condition them for freeze-thaw testing. These specimens, with measured dry masses, were place in the vacuum desiccators with a vacuum pump running to achieve 1 in. air pressure (~ 28.5 in. Hg of vacuum), then they were inundated with water-ethanol solution (with a concentration of 0.5% ethanol) without breaking the vacuum and left in the solution under the vacuum for 15 minutes. Following this, each aggregate fraction specimen was placed in a plastic container under ¼ in. of water-ethanol, covered, and placed in an automated freeze-thaw test system that conforms to AASHTO T 103 freeze-thaw cycle requirements, as shown in Figure 3.4. In order to investigate the current freezing-thawing practices on the results of freeze-thaw testing of coarse aggregates, the samples were divided into two sets of duplicate aggregate sources. Each set had nine duplicate coarse aggregate types which were fractioned, resulting in a total of 36 specimens in each set. The specimens were subjected to the freeze-thaw cycles. One set was placed in the automated freezer system and the other set was placed in a commercial grade chest freezer (manual freeze-thaw cycles). Sample preparation and conditioning was the same for the specimens processed in both the automated freeze-thaw system and the chest freezer. The freezing and thawing temperature requirements of the AASHTO T 103 standard procedure were satisfied during the freeze-thaw cycles using the chest freezer.

The coarse aggregate fraction specimens placed in the automated system were kept for eight continuous day to complete 16 freeze-thaw cycles (six hours of freezing and six hours of

thawing were enough to satisfy the temperature requirements). On the other hand, the coarse aggregate fraction specimens placed in the chest freezer needed 16 days of continuous testing to complete the 16 freeze-thaw cycles. It should be noted that the chest freezer experience was not easily performed, and the testing required inconsistent working times. Observation of the freezer temperature indicated that freezing times were inconsistent. A data acquisition system with thermocouples connected to the inside of a coarse aggregate particle inside the plastic container was used to monitor and verify the test temperature when the chest freezer was used. The freezing cycle time ranged between eight and twelve hours to achieve the temperature requirement, and the thawing cycle time varied between four and six hours when the chest freezer was used.

After the completion of the 16th cycle, each specimen was washed, oven-dried, and sieved on the appropriate sieve size. The retained mass of each specimen was measured and recorded, and the mass loss was calculated.

Figure 3.4: Freeze-thaw test system used to process the investigated coarse aggregates

3.2 Coarse Aggregates in Portland Cement Concrete

Three coarse aggregate samples, one calcareous (CLS11) and two dolomitic limestone (DLS4 and DLS7), collected from different quarries, were used to design Portland cement concrete mixes following WisDOT mixture design requirement for PCC pavement surface. The other mixture ingredients (i.e., the fine aggregates, Portland cement, fly ash, air entraining and admixtures, etc.) were all kept the same for all three PCC mixes. The mixing of PCC, quality control testing, preparation/casting of 4 in. and 6 in. diameter cylinders, and the curing were conducted by Titi et al. (2022) and the Trierweiler Construction & Supply Co., Inc. at the latter's PCC laboratory in Marshfield, WI. Figure 3.5 depicts the PCC mixing, test cylinders preparation, and curing. The coarse aggregate CLS9 was used in a WisDOT approved PCC mix by a paving contractor, who provided the 4 in. PCC cylinders. PCC mixture constituents and properties used to make the test cylinders in this study are presented in Tables 3.3 and 3.4.

Table 3.3: Portland cement concrete mixture proportions used to create concrete cylinders

Material	Source	Weight (lbs)	Actual R.D.	Volume
Cement	Alpena	395	3.15	2.01
Fly Ash	Portage	170	2.76	0.98
Slag		0	0.00	0.00
Coarse A		0	1.00	0.00
Fine	Sand	1258	2.68	7.53
Coarse B	CLS11	1887	2.65	11.42
Not Used		0	1.00	0.00
Not Used		0	1.00	0.00
Water	Well	215	1.00	3.44
Air %		6.0		1.62
TOTAL		3925		27.00

Table 3.4: PCC mixture properties

Coarse aggregate	Water/Cement Ratio	Air content (%)
CLS9	0.45	5.1
CLS11	0.40	5.7
DLS4	0.39	4.6
DLS7	0.39	4.7

Figure 3.5: Picture of the various steps taken to prepare PCC test cylinders.

The laboratory testing regimen for this study was conducted on concrete cylinders that contained coarse aggregate from sources CLS11, DLS4, and DLS7. The testing performed on the concrete cylinders consisted of: ASTM C666 *Standard Test Method for Resistance of Concrete to Rapid Freezing and Thawing*, ASTM C215 *Standard Test Method for Fundamental Transverse, Longitudinal, and Torsional Resonant Frequencies of Concrete Specimens*, ASTM

C597 *Standard Test Method for Pulse Velocity Through Concrete*, and ASTM C39 *Standard Test Method for Compressive Strength of Cylindrical Concrete Specimens.*

3.2.1 Resistance of Concrete to Rapid Freezing and Thawing

The PCC cylinders prepared using the investigated coarse aggregates (4 in. by 8 in.) were used to evaluate the freeze-thaw durability of the PCC used in pavement surface layers. A group of these cylinders were prepared using the same exact mix design and mixture constituents, and only varying the coarse aggregate type/source. The other group was obtained from a pavement construction site during paving operation and was cast by a certified technician. These concrete cylinders were cured for 28 days and then kept in a dry state on a shelf in the laboratory for six months. After six months, these cylinders were subjected to rapid freeze-thaw cycles in accordance with the ASTM C666 standard test procedure B, but with a modification of the freeze-thaw cycle time and sample size. It was not possible to reach the temperature ranges required in ASTM C666 standard procedure in the middle of the concrete samples within the time limits specified. On average, seven hours were needed to achieve the temperature ranges. In addition, the samples used were the 4 in. by 8 in. cylinders. The research objective is to evaluate the performance of the PCC based on the influence of the coarse aggregate type. Since all investigated samples were subjected to the same test conditions, the relative performance of the PCC and the coarse aggregate used to produce it can still be evaluated with such modification to the ASTM C666 standard test procedure.

The investigated concrete samples were subjected to 300 freeze-thaw cycles. However, a limited number of specimens were tested to 450 freeze-thaw cycles. Pictures of the concrete samples in the freeze-thaw chamber are shown in Figure 3.6.

(a)

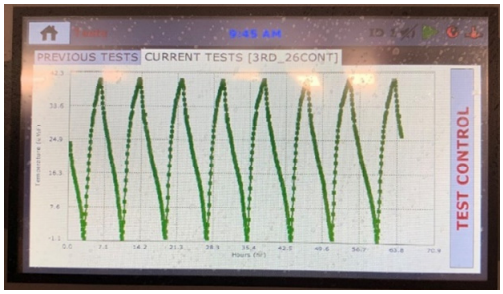

(b)

Figure 3.6: (a) PCC cylinders in frozen state inside the rapid freeze-thaw chamber; (b) The temperature-time freeze-thaw cycles applied to these cylinders

3.2.2 Evaluation of PCC Properties due to Rapid Freeze-Thaw Cycles

In order to investigate the influence of coarse aggregate quality on PCC performance, the dynamic modulus of elasticity was evaluated for the PCC cylinders after the completion of a certain number of freeze-thaw cycles. The number of cycles varied but was generally about every 30 freeze-thaw cycles.

The dynamic modulus of elasticity (E_d) of the PCC cylinders was determined using the impact resonance frequency method in accordance with ASTM C215 *Standard Test Method for Fundamental Transverse, Longitudinal, and Torsional Resonant Frequencies of Concrete Specimens*. In this this method, the fundamental resonant frequencies (longitudinal and transverse) of the tested specimen were measured, as depicted in Figure 3.7. The 4 in. diameter

PCC cylinders were tested using a commercially available system with a software for signal processing,

Prior to placing the PCC cylinders in the freeze-thaw chamber, the resonant frequency testing was performed on three cylinders to establish the values of the dynamic elastic modulus (E_{d0}) before any freeze-thaw cycles are applied to the PCC. The PCC cylinders were removed from the freeze-thaw chamber approximately every 30 cycles to perform resonant frequency testing on the cylinders and then placed again in the freeze-thaw chamber after changing the water in the container.

In addition, the dynamic elastic modulus for the investigated PCC cylinders was determined through the ultrasonic pulse velocity (UPV) testing in accordance with ASTM C597 *Standard Test Method for Pulse Velocity Through Concrete*. The purpose of the UPV method is to measure the travel time of ultrasonic pulse waves that travel through the PCC cylinders. The dynamic modulus of elasticity was calculated using the UPV, cylinder dimensions, and weight.

The ultrasonic pulse was propagated through the concrete cylinders with a pulse generator and measured with a receiving circuit. The pulse wave was additionally measured with an oscilloscope to increase accuracy of the measurement. Figure 3.7 depicts a set of images for the stiffness and strength tests conducted on the investigated PCC cylinders.

(a) Longitudinal resonant frequency test of PCC cylinder

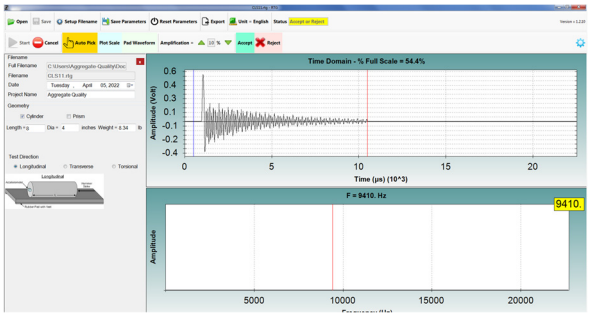

(b) Software for signal perocessing

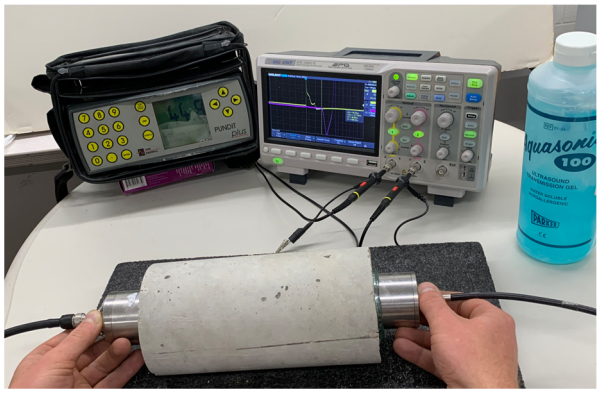

(c) Ultrasonic pulse velocity test of PCC cylinder

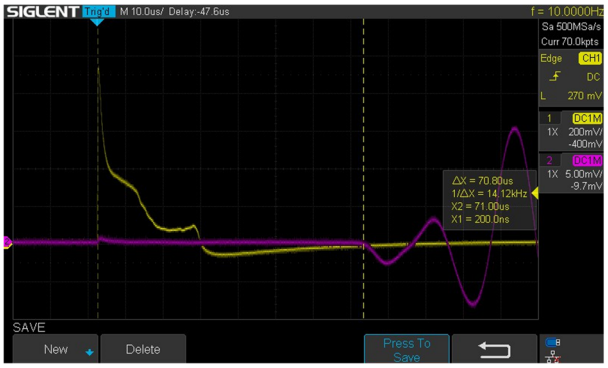

(d) Oscilloscope for signal processing

Figure 3.7: Laboratory tests used to evaluate the PCC stiffness and strength properties due to freeze-thaw cycles.

Chapter 4

Test Results, Analysis, and Evaluation

This chapter presents the results of the laboratory tests conducted on the unbound coarse aggregates. The results include specific gravity, absorption, vacuum absorption, and mass loss due to sodium sulfate and freeze-thaw tests. Additionally, tests performed on the PCC cylinders made with three coarse aggregate sources to evaluate the stiffness and strength of the PCC due to freeze-thaw conditioning. A critical analysis and evaluation of the test results is also attempted in this chapter.

4.1 Coarse Aggregates Test Results and Evaluation

4.1.1 Specific Gravity

The results of AASHTO T 85 test used to determine the specific gravity of the investigated coarse aggregates are depicted in Figure 4.1. The bulk specific gravity of the calcareous limestone aggregates ranges from 2.40 to 2.64 with an average of 2.55 and the bulk specific gravity of the dolomitic limestone varies between 2.60 and 2.77 with an average of 2.73. The results show that the calcareous limestone aggregate possessed bulk specific gravity values less, on average, compared with the dolomitic limestone. In addition, the difference between the bulk specific gravity and the apparent specific gravity for the calcareous limestone coarse aggregates is larger than that of the dolomitic limestone, demonstrating that the calcareous limestone aggregates are more porous than the dolomitic limestone aggregates. The bulk specific

gravity, the saturated-surface dry specific gravity, and the apparent specific gravity values are generally within the typical ranges of aggregates of fine-grained, sedimentary rock origin.

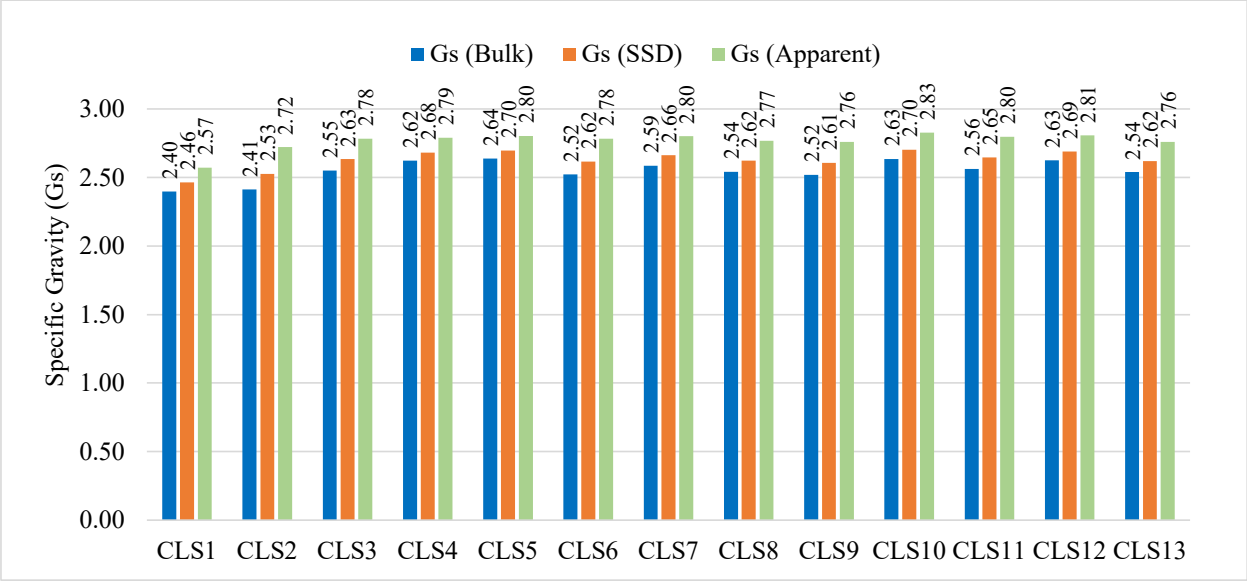

(a) calcareous limestone coarse aggregate samples

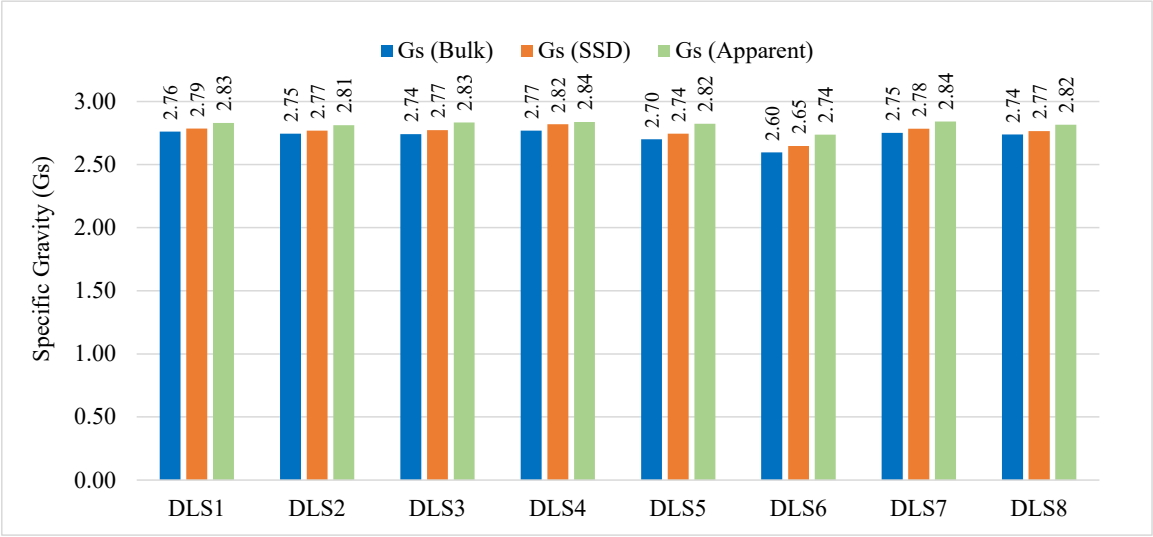

(b) dolomitic limestone coarse aggregate samples

Figure 4.1: Specific gravity (G_s) values for the investigated coarse aggregate samples

4.1.2 Absorption and Vacuum Absorption

The results of the AASHTO T 85 and MDOT MTM 113 tests to determine the absorption and vacuum absorption values of the investigated coarse aggregates, respectively, are shown in Figure 4.2. The results are for the size fractions retained on $^{3}/_{8}$ in. and ½ in. sieves. Inspection of Figure 4.2 shows that the vacuum absorption values of the investigated coarse aggregates, with an average of 2.50%, are greater that the absorption values, with an average of 2.04%. In addition, the test results indicate that the dolomitic limestone coarse aggregate possessed absorption values (average of 1.07%) are less than those of the calcareous limestone (average of 2.71%).

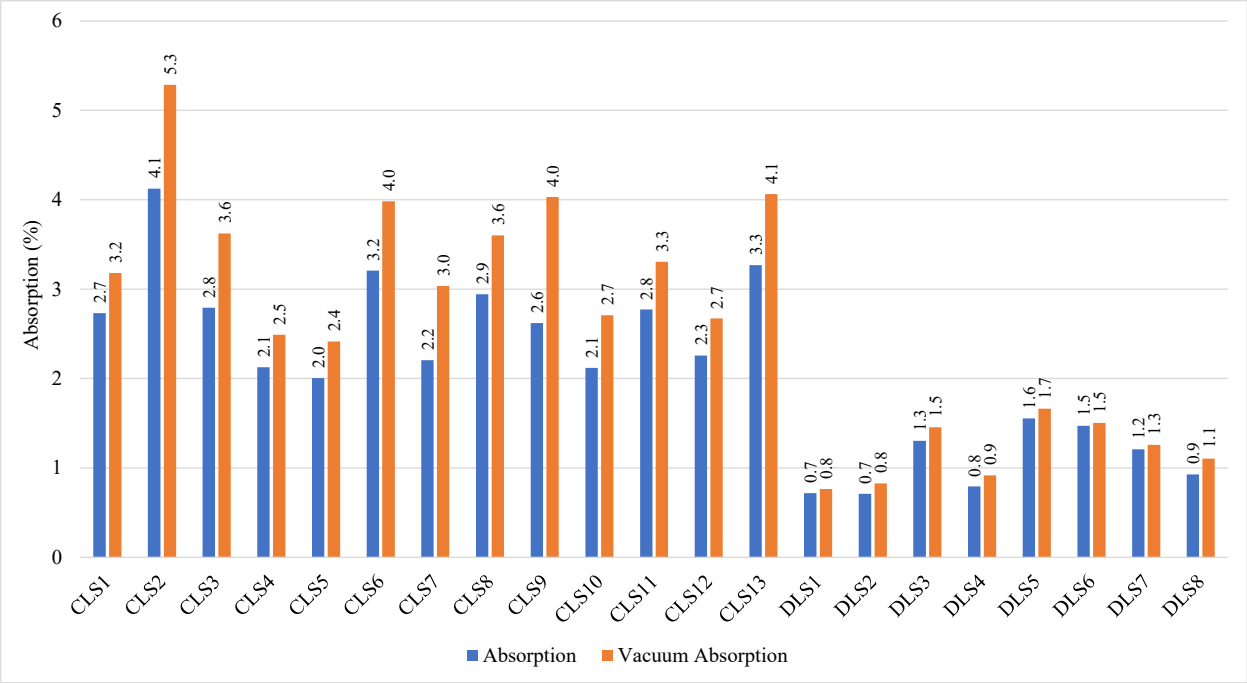

(a) weighted average for ½ in. and 3/8 in. size fractions

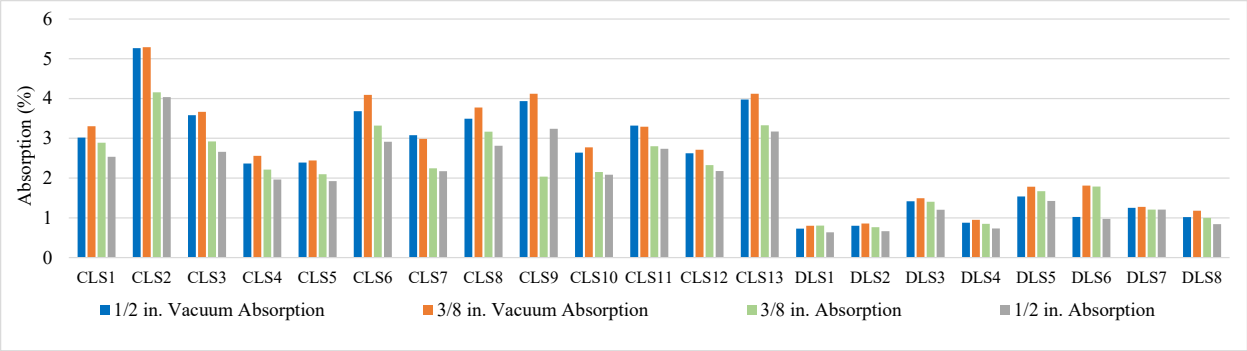

(b) ½ in. and 3/8 in. size fractions

Figure 4.2: Absorption and vacuum absorption test results of the investigated coarse aggregates (a) weighted average for 1/2 in. and 3/8 in. size fractions, and (b) ½ in. and 3/8 in. size fractions

Titi et al. (2022) conducted statistical analysis on a large dataset of absorption test results of coarse aggregates from various Wisconsin rock formations as shown in Figure 4.3. The dataset minimum and maximum absorption values of the coarse aggregate in the dataset are 0.126% and 4.95%, respectively, with an average of 1.88% and standard deviation of 0.887%. The coarse aggregates investigated in this study possessed an average absorption value of 2.04%, which corresponds to approximately 45.6% of the coarse aggregates in the dataset. This shows that the absorption values of the investigated aggregates, on average, are relatively high. Calcareous limestone coarse aggregates usually have relatively high porosity due to the porous nature of calcareous limestone.

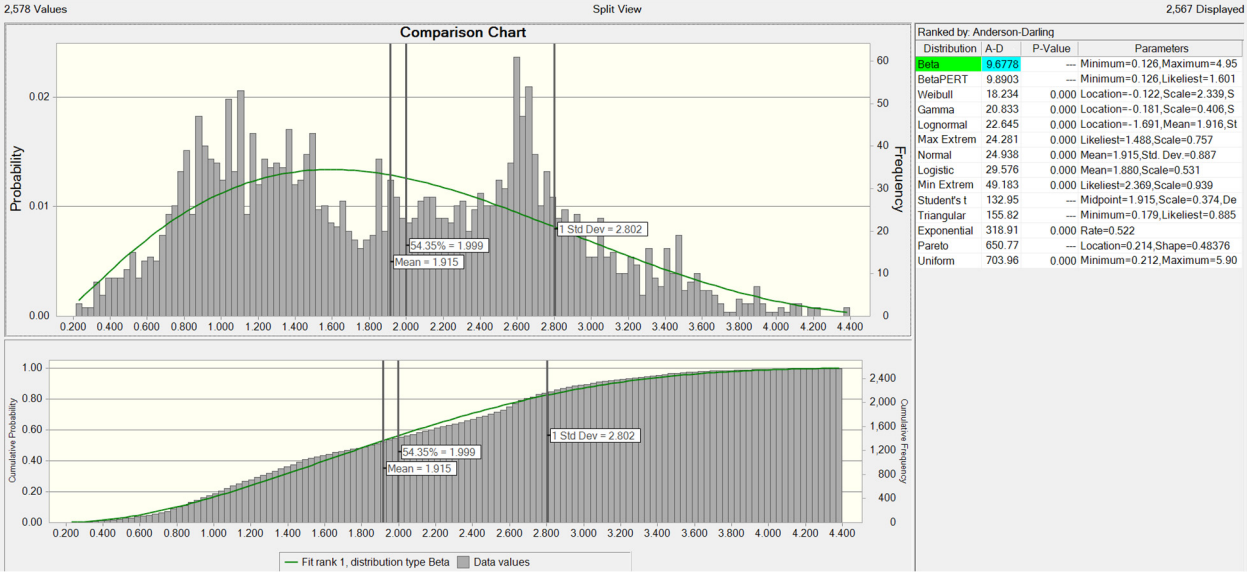

Figure 4.3: Results of statistical analysis on a large dataset of absorption tests conducted on Wisconsin aggregates of various rock formations (after Titi et al. 2022)

Examination of Figure 4.3 shows that the distribution of the absorption data is bimodal. The bimodal distribution of the data is split into two separate distributions, as shown on Figure 4.4. This is attributed to the presence of two groups of coarse aggregates. One group has relatively low absorption values that are typically obtained from igneous and metamorphic rocks such as granite and quartzite formation, in addition to some low porosity types of dolomitic limestone (which is a sedimentary rock). The other group consists of aggregates collected from formations with relatively high absorption values such as calcareous limestone with high porosity and some dolomitic limestone formations that possess relatively high porosity.

The absorption data of the investigated 13 calcareous limestone coarse aggregate samples fell within the second group with an average absorption value of 2.64% and the eight dolomitic coarse aggregate fell within the first group with an average absorption value of 1.13%.

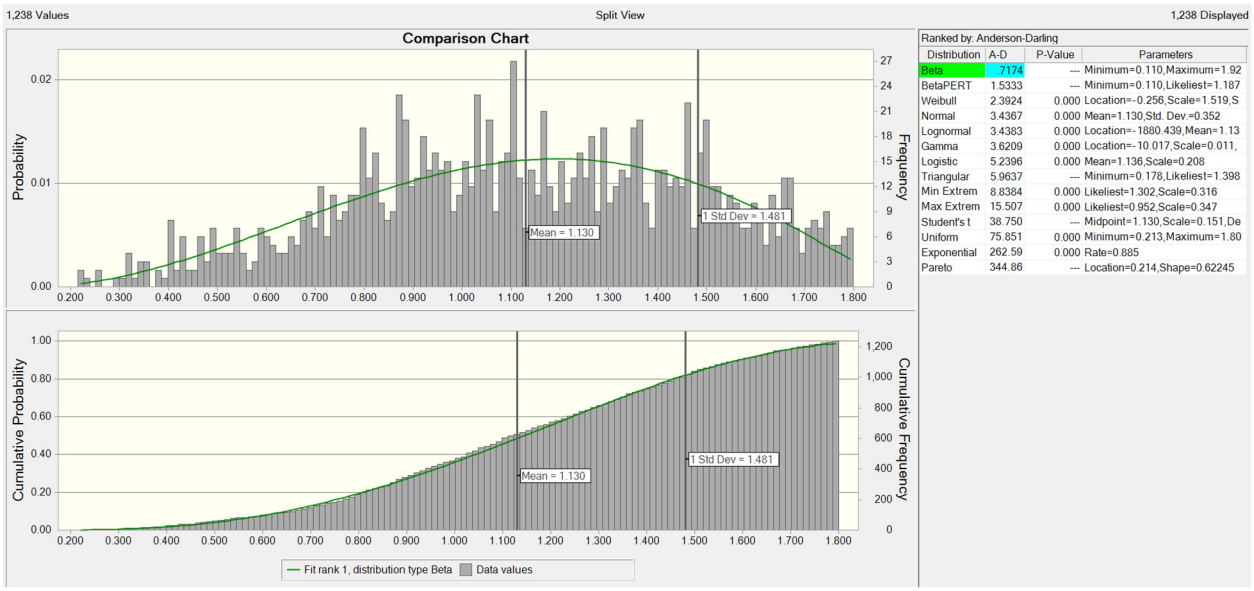

(a)

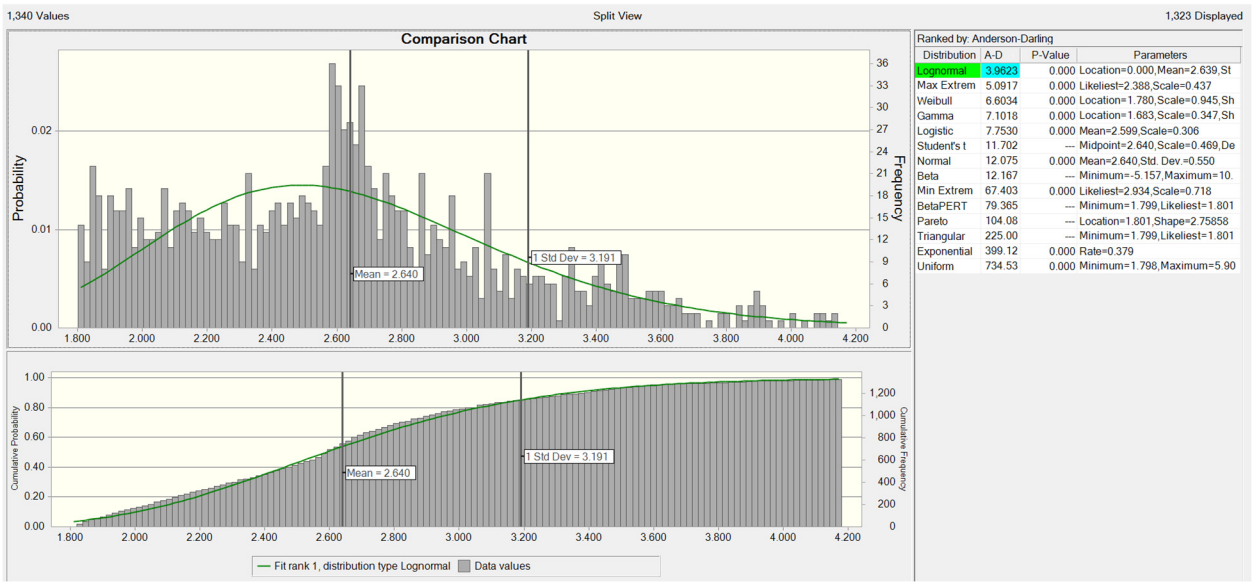

(b)

Figure 4.4: Bimodal distribution of absorption testing of Wisconsin dataset

4.1.3 Sodium Sulfate and Freeze-Thaw

The results of the sodium sulfate soundness test for the investigated coarse aggregate samples are shown in Figure 4.5. The percent mass loss of the investigated coarse aggregates varied between 1.0% and 28.5% for the dolomitic limestone and between 4.0% to 24.8% for the calcareous limestone. The average mass loss from sodium sulfate soundness testing of the investigated coarse aggregates is 15.06%.

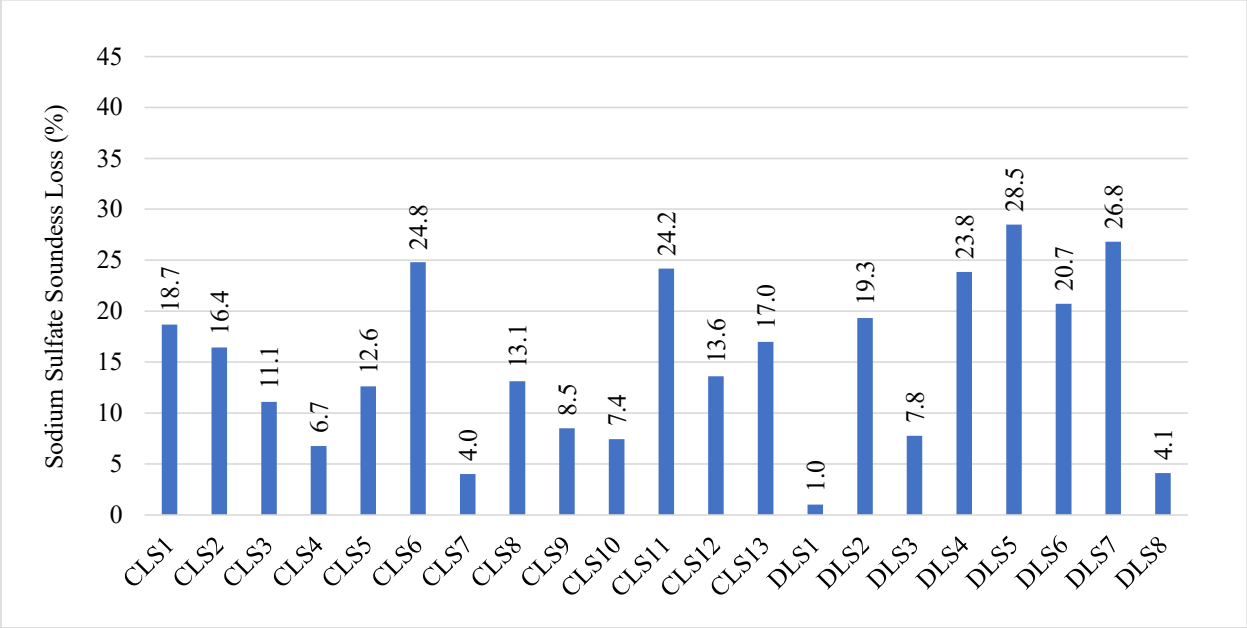

Figure 4.5: Total sodium sulfate soundness loss

Titi et al. (2022) conducted comprehensive statistical analysis on sodium sulfate and freeze thaw tests conducted on Wisconsin aggregates as presented in Figures 4.6 and 4.7 Inspection of Figure 4.5 shows that if 7% of the evaluated aggregate samples would fail the sodium sulfate soundness test, the corresponding cut-off mass loss percentage is 11.8% (measured using the sodium sulfate soundness test). When comparing the investigated coarse aggregate sodium sulfate soundness mass loss to the large data set analyzed by Titi et al. (2022), eight out of the thirteen calcareous limestone specimens possessed a percent loss values greater

than 11.8% and five out of the eight dolomitic limestone samples exhibited sodium sulfate percent mass loss larger than 11.8%. The relatively large population of higher mass loss percentage indicates that the investigated coarse aggregates possessed physical properties related to porosity, pore size, and pore size distribution, that resulted in high absorption values and subsequently influenced the durability of aggregate. In addition, a number of the investigated aggregate sources are of poor to marginal quality with non-formation material.

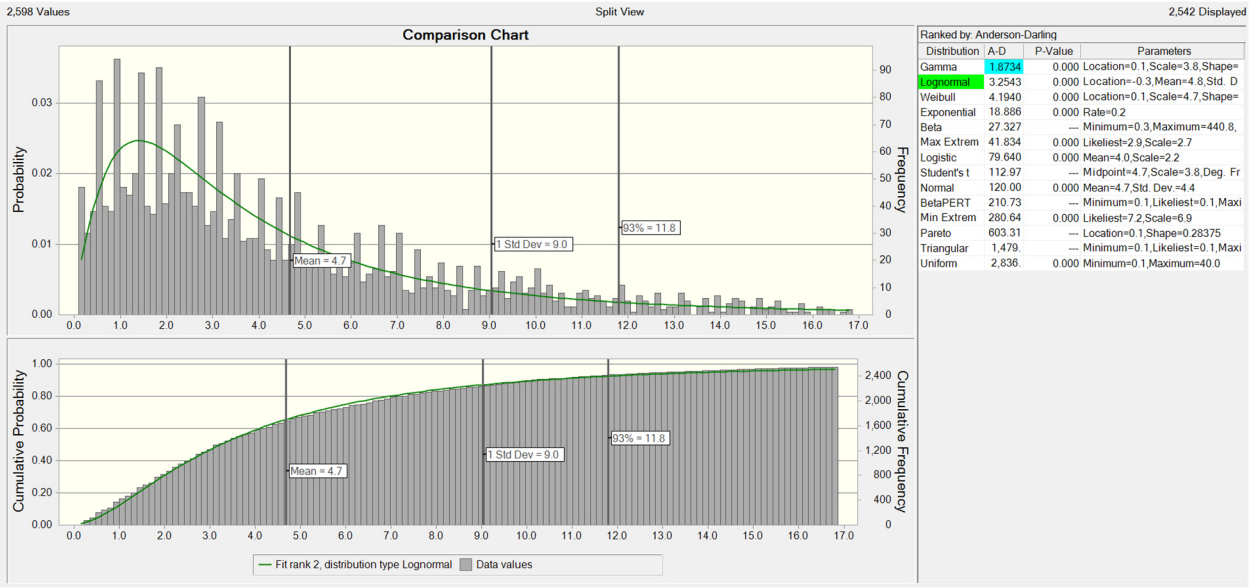

Figure 4.6: Results of statistical analysis on a large dataset of sodium sulfate soundness tests conducted on Wisconsin aggregates of various rock formations (after Titi et al. 2022)

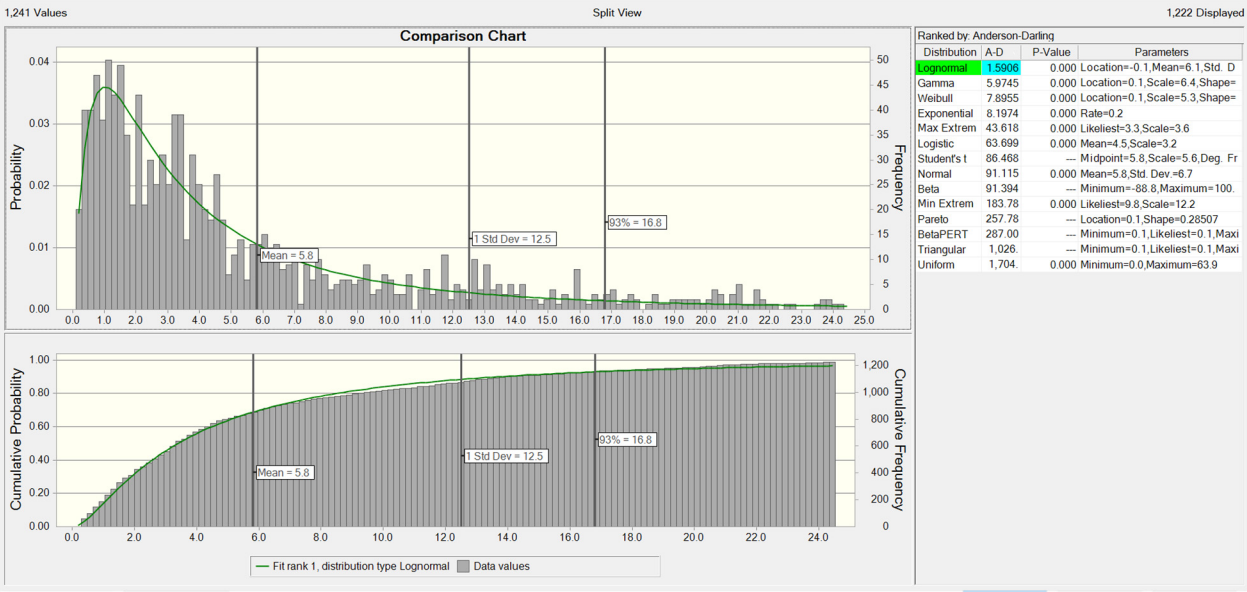

Figure 4.7: Results of statistical analysis on a large dataset of freeze-thaw tests conducted on Wisconsin aggregates of various rock formations (after Titi et al. 2022)

As presented and discussed in Figure 4.5, the results of sodium sulfate soundness test percent mass loss of the investigated coarse aggregates varied between 1.0% and 28.5%. There is no specific trend when comparing calcareous versus dolomitic limestone. Both calcareous and dolomitic limestone coarse aggregates exhibited relatively low and high values of percent mass loss. The relationship between sodium sulfate mass loss and absorption as well as vacuum absorption of the investigated coarse aggregates are shown in Figure 4.8. While R^2 (coefficient of determination) values are reasonable (R^2= 0.65 for absorption and R^2= 0.63 for vacuum absorption), the author believes this is not representative of the broader set of Wisconsin coarse aggregates due to the nature of aggregate porosity and the pore size distribution of the studied aggregates. There are coarse aggregates with high absorption (porosity) that exhibited low sodium sulfate soundness mass loss and vice versa.

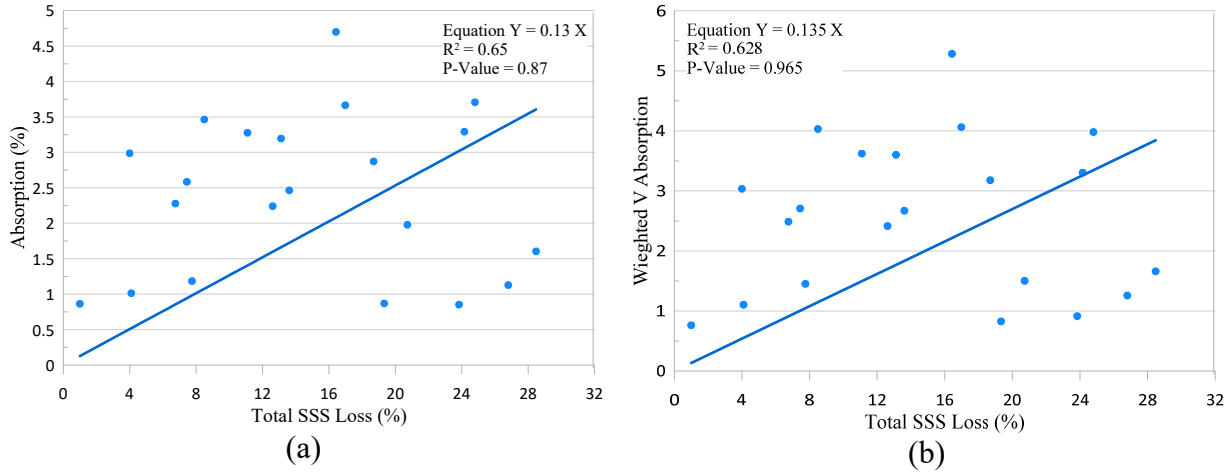

Figure 4.8: (a) Total absorption vs. total sodium sulfate loss (b)Weighted vacuum absorption vs. total sodium sulfate loss

In addition, the dolomitic and the calcareous limestone coarse aggregate samples contain non-formation particles such as shale, chalk, chert and other materials that influence the results of the mass loss if present in the tested specimen Figure 4.9 depicts particles that are considered non-formation within the coarse aggregate tested specimens showing significant degradation/breakage and disintegration due to sodium sulfate wetting/drying cycles.

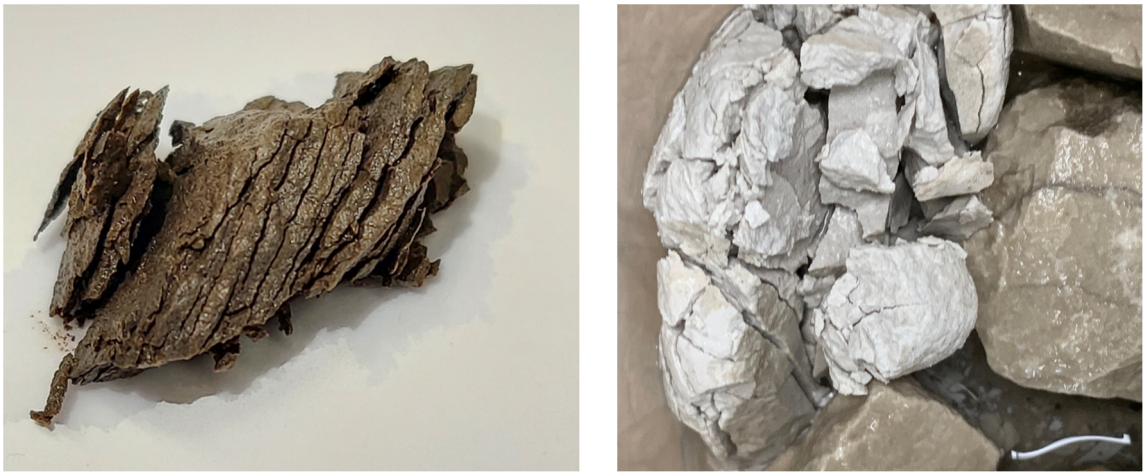

(a) shale from dolomitic limestone aggregate sample

(b) chalk aggregate in calcareous limestone aggregate sample

Figure 4.9: Non-formation particles within tested coarse aggregate specimens

The results of the freeze-thaw soundness test for the investigated coarse aggregate samples are shown in Figure 4.10. The percent mass loss of the investigated coarse aggregates varied between 4.1% and 41.2% for the dolomitic limestone and between 2.1% to 31.3% for the calcareous limestone. It should be noted that the average mass loss of the investigated coarse aggregates is 14.9%.

In general, the dolomitic limestone coarse aggregates exhibited a higher mass loss versus the calcareous limestone. This difference is attributed to the presence of non-formation particles present in the tested specimens, such as shale, as discussed earlier. When comparing the test results of the investigated coarse aggregates with the Wisconsin aggregate data analyzed by Titi et al. (2022), as shown in Figure 4.7, three out of thirteen calcareous limestone samples exhibited a mass loss due to freeze-thaw test greater than 16.8%, which corresponds to 93% passing specimens out of the large test population (remaining consistent with the previous 7% failure used for the sodium sulfate dataset analysis). For the dolomitic limestone five out of eight samples possessed a freeze-thaw mass loss greater than 16.8%. It should be noted that the five dolomitic limestone specimens that failed the large set threshold limit of 11.8% for the sodium sulfate soundness test are the same coarse aggregate samples that failed the freeze-thaw threshold limit of 16.8% based on the analysis of the large data set.

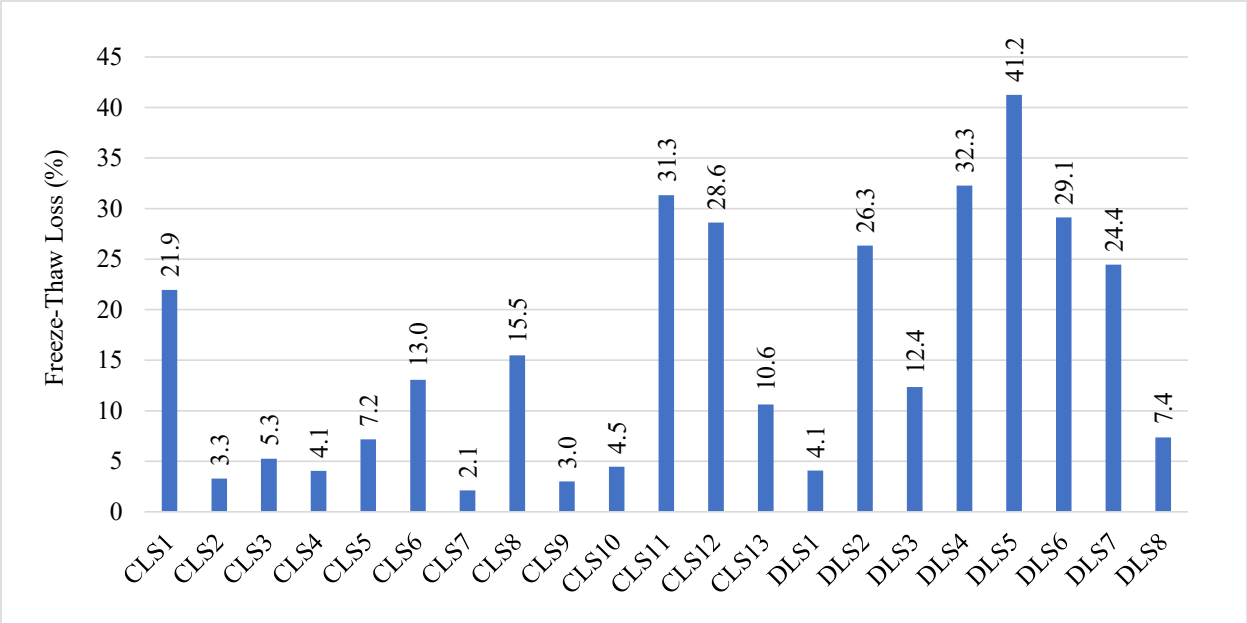

Figure 4.10: Total freeze-thaw mass loss

The relationship between freeze thaw mass loss and absorption of the investigated coarse aggregates is shown in Figure 4.11. The R^2 value based on the conducted testing is 0.40 which appears to be reasonable. As previously noted, the sample size is not considered representative of the broader set of Wisconsin limestone coarse aggregates and it is recommended that additional duplicate testing be performed and datasets be analyzed to better understand this relationship.

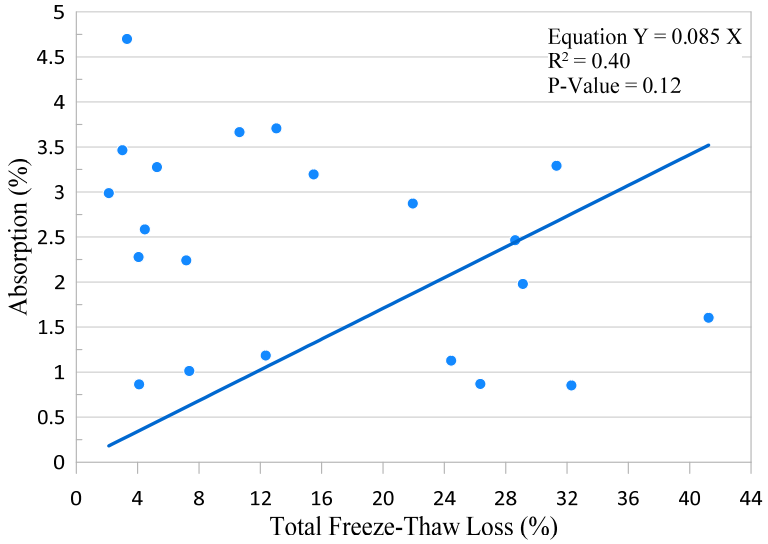

Figure 4.11: Absorption vs. total freeze-thaw loss

A comparison of the results total sodium sulfate soundness test mass loss and total freeze-thaw test mass loss is shown in Figure 4.12. Observation of Figure 4.12 indicates that the sodium sulfate soundness loss was generally greater than the freeze-thaw loss for calcareous limestone coarse aggregates, and the sodium sulfate soundness loss was generally less than the freeze-thaw loss for dolomitic limestone coarse aggregates.

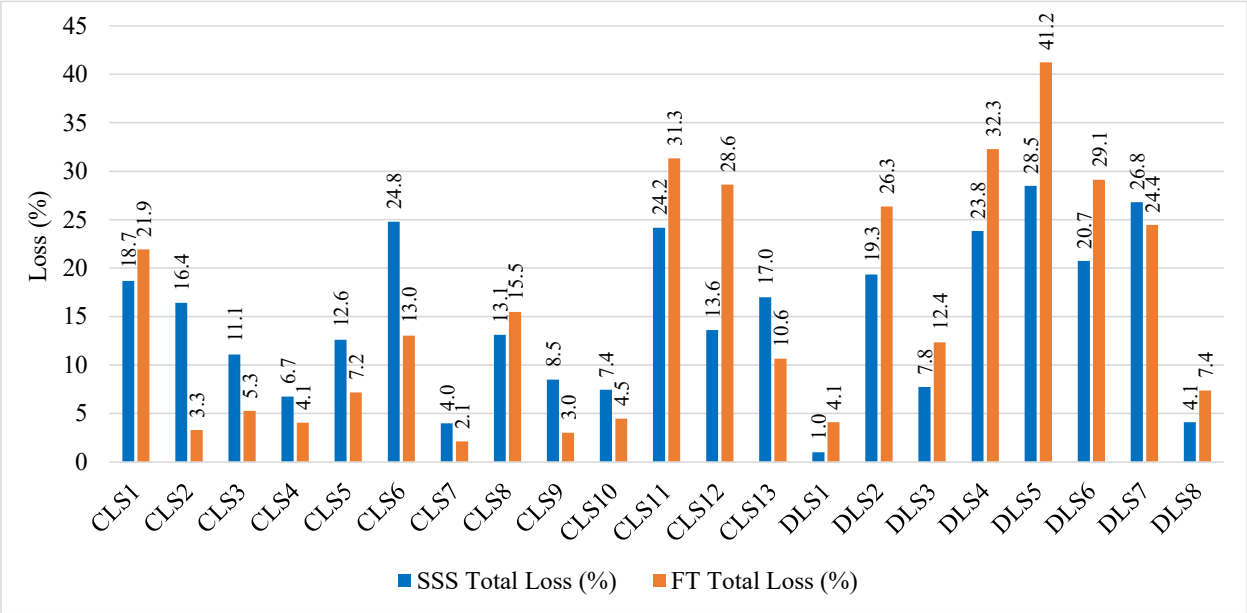

Figure 4.12: Comparison of sodium sulfate total loss and freeze-thaw total loss

The relationship between the total freeze-thaw loss and sodium sulfate soundness of the investigated coarse aggregates are shown in Figure 4.13. The R^2 of this relationship was relatively high (R^2= 0.86). However, based on the limited size of this dataset and considering that the studied aggregates were all relatively marginal in terms of freeze-thaw performance, this relationship is not considered representative of the broader set of Wisconsin limestone coarse aggregates. Due to the presence of non-formation particles encountered in several aggregates and considering the porosity and pore size distribution of the studied aggregates, the selected samples

may show a strong relationship between sodium sulfate soundness, which is not believed to translate to a larger dataset of Wisconsin limestone aggregates.

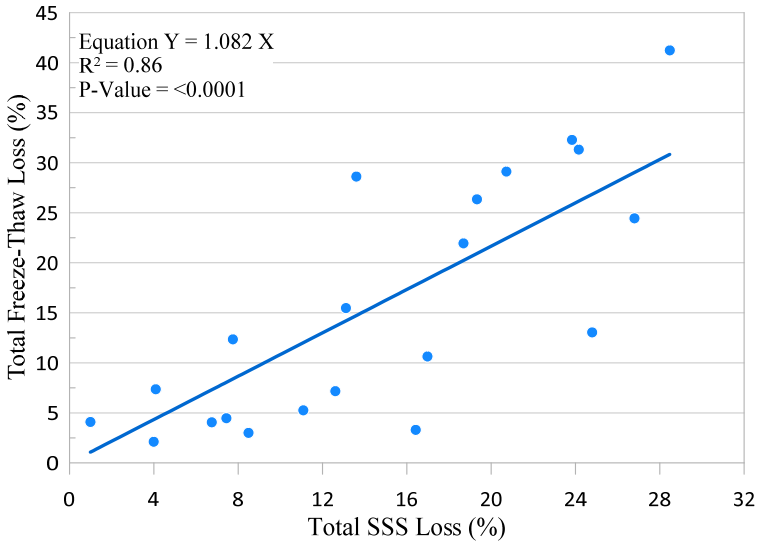

Figure 4.13: Total freeze-thaw loss vs. total sodium sulfate soundness loss

Freeze-thaw testing was performed on fractions 3/8 in. and ½ in. size fractions of the coarse aggregates. Investigation of the percent mass loss of the 3/8 in. and ½ in. size fractions showed greater mass loss exhibited by the smaller size fraction, 3/8 in., than that of the ½ in. The fractioned mass loss from freeze-thaw testing is shown in Figure 4.14. The average loss of the investigated 3/8 in. aggregate fractions was 19.1% and the average loss of the investigated ½ in. aggregate fractions was 10.0%.

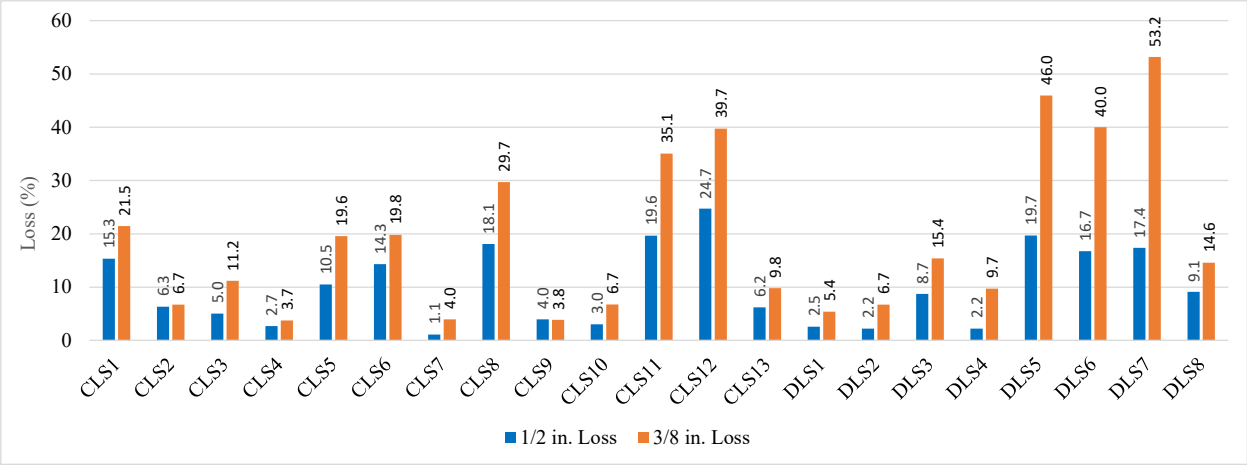

Figure 4.14: Comparison of 3/8 in. and ½ in. coarse aggregate fraction loss from freeze-thaw testing

Freeze-thaw testing in accordance with AASHTO T 103 was performed on select coarse aggregate samples with a commercially available chest freezer and with an automated freezer system. Weighted average loss of each method is presented in Figure 4.15. Figure 4.15 indicates no clear relationship between the chest freezer and automated freeze-thaw machine methods.

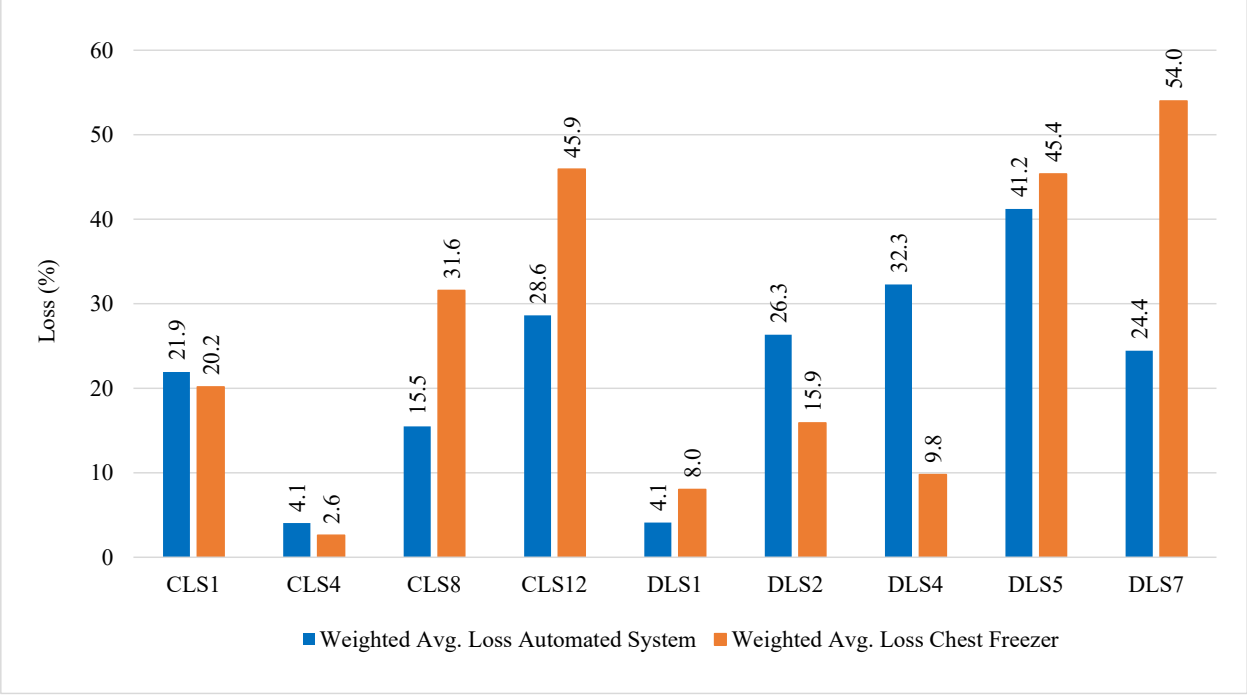

Figure 4.15: Comparison of weighted average loss for chest freezer and automated freezer system freeze-thaw testing on coarse aggregates

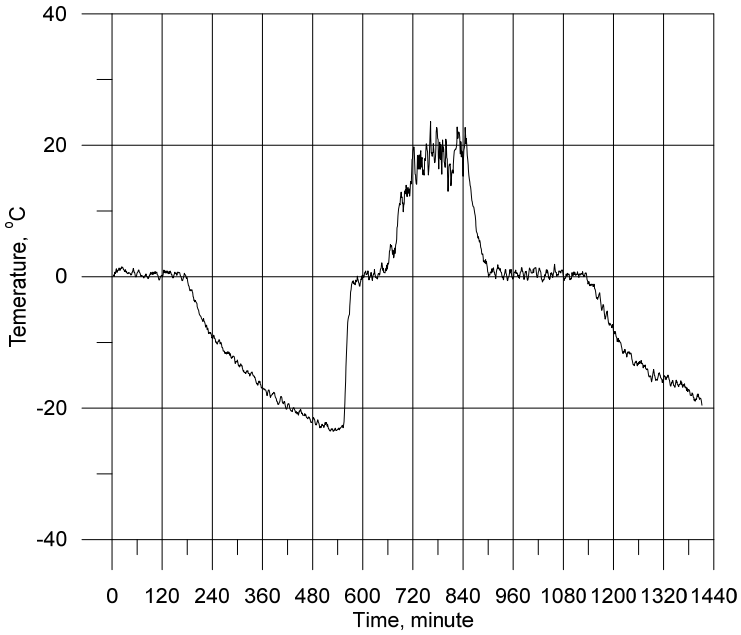

Figure 4.16: Temperature-time graph of chest freezer freeze-thaw test cycle

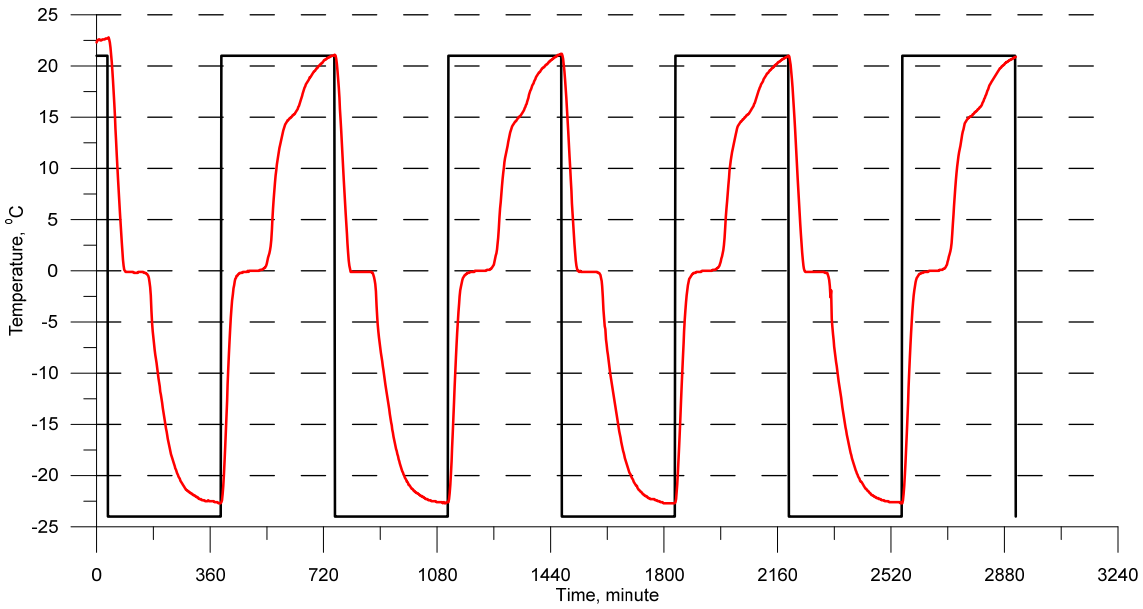

Figure 4.17: Temperature-time graph of automated freezer system freeze-thaw test cycles (black line indicates the freezer temperature input; red line indicates the measured temperature)

The measured temperature-time graphs for the chest freezer method and automated freezer system methods are shown in Figures 4.16 and 4.17, respectively. Observation of Figures 4.16 and 4.17 indicates that one freeze-thaw cycle for a chest freezer was approximately 16 hours (which varied throughout testing depending on the measured freezing rate) whereas, one freeze-thaw cycle for the automated system was approximately 12 hours. It should be noted that the automated system provided a greater ease of use over the chest freezer. Testing was programmed and automatically run, compared with the chest freezer, where inconvenient testing times were required to place and remove samples from the chest freezer.

During the chest freezer freeze-thaw testing, careful effort was made not to disturb the samples during movement to and from the chest freezer when samples were removed or placed in the freezer, but samples were still mechanically disturbed during movement. The freeze-thaw time and rate in the chest freezer was variable and found to be inconsistent through different cycles. Additionally, measurements of different locations of the chest freezer during the freezing portion of the test showed different temperatures. The location of the specimen in the chest freezer was impacted by variability of temperature. These factors induced a higher variability to the test method and may have affected the results of the chest freezer freeze-thaw test, compared to the automated freeze-thaw machine.

4.2 Portland Cement Concrete Test Results and Evaluation

4.2.1 Resistance of Concrete to Rapid Freezing and Thawing

Results of the ASTM C666 procedure are presented in Figures 4.17 for the relative longitudinal and transverse dynamic modulus values of the tested concrete cylinders throughout the test cycles. The reported relative dynamic modulus values (E_d/E_{d0}) are the ratio of the measured dynamic modulus tested during rapid freeze-thaw testing to the final tested dynamic modulus of a control sample at the end of the tested cylinder's freeze-thaw testing.

Inspection of Figures 4.18 for the relative longitudinal and transverse dynamic modulus values over time indicate that only the DLS11 cylinders dropped below 0.9 relative dynamic modulus after 300 freeze-thaw cycles, and the remaining samples were all above 0.9. These results indicate that the tested aggregates in concrete generally have a high resistance to freeze-thaw cycles after 300 cycles. It should also be noted that during the freeze-thaw cycles, the relative dynamic longitudinal and transverse modulus increased for several samples. The increase in ratio is likely due to the cylinders continuing to cure during the thawing phases of the freeze-thaw cycle.

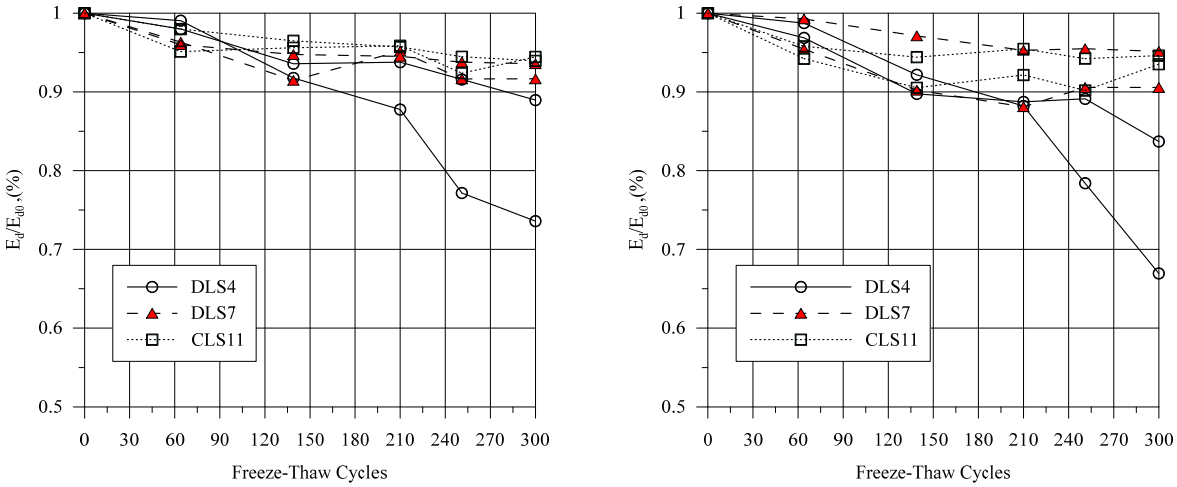

(a) longitudinal E_d (b) transverse E_d

Figure 4.18: Relative dynamic modulus vs. time

4.2.2 Ultrasonic Pulse Velocity Testing of PCC Cylinders

Ultrasonic pulse velocity (UPV) testing, in accordance with ASTM C597, was performed on the concrete cylinders to determine the dynamic modulus of elasticity. Graphical results of the dynamic elastic modulus, measured through UPV testing are presented in Figure 4.18. Samples were tested at the conclusion of 300 freeze thaw-cycles. Additionally, dynamic modulus of the control samples for each cylinder (labeled as -V) was tested in both a saturated and oven-dry state at the same time as the freeze-thaw tested samples. Inspection of Figure 4.19 indicates that for each cylinder type (CLS11, DLS4, and DLS7), the E_d (saturated) was greater than the E_d (dry) for the control samples. Also, the saturated and dry control sample E_d values were greater than the E_d value at the conclusion of 300 cycles of freeze thaw testing.

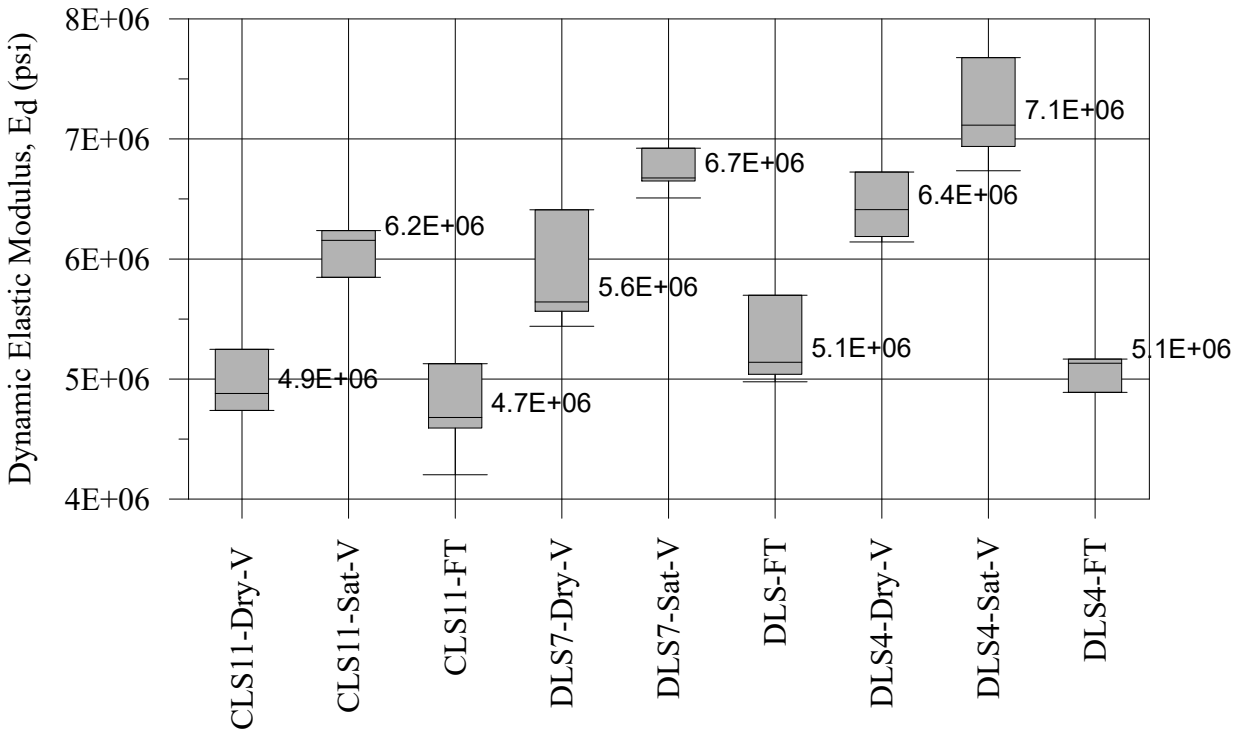

Figure 4.19: Dynamic elastic modulus of PCC cylinders measured through UPV

4.2.3 Compressive Strength of PCC

Compressive strength testing was performed on the PCC cylinders in accordance with ASTM C39. Results of the compressive strength testing are shown in Figure 4.20. The compressive strength (f_c') was 6,840 psi for the DLS4-2 cylinder, and the minimum f_c' was 5,191 for the DLS4-1 PCC cylinder. The average compressive strength of CLS11 and DLS7 freeze-thaw tested PCC cylinders was less than the control compressive strength PCC cylinders for those aggregates. The average compressive strength for of the DLS4 freeze-thaw tested cylinder was larger than the average compressive strength of the control DLS4 PCC cylinders.

The elastic modulus values of the PCC cylinders were estimated using Equation 4 in Section 19.2.2 ACI 318-14 (ACI, 2014). Results of the estimated modulus of elasticity values are presented in Figure 4.21. The estimated modulus of elasticity values were averaged for the control and freeze-thaw tested PCC cylinders. A comparison of the average modulus of elasticity for the control and tested samples is presented in Figure 4.22.

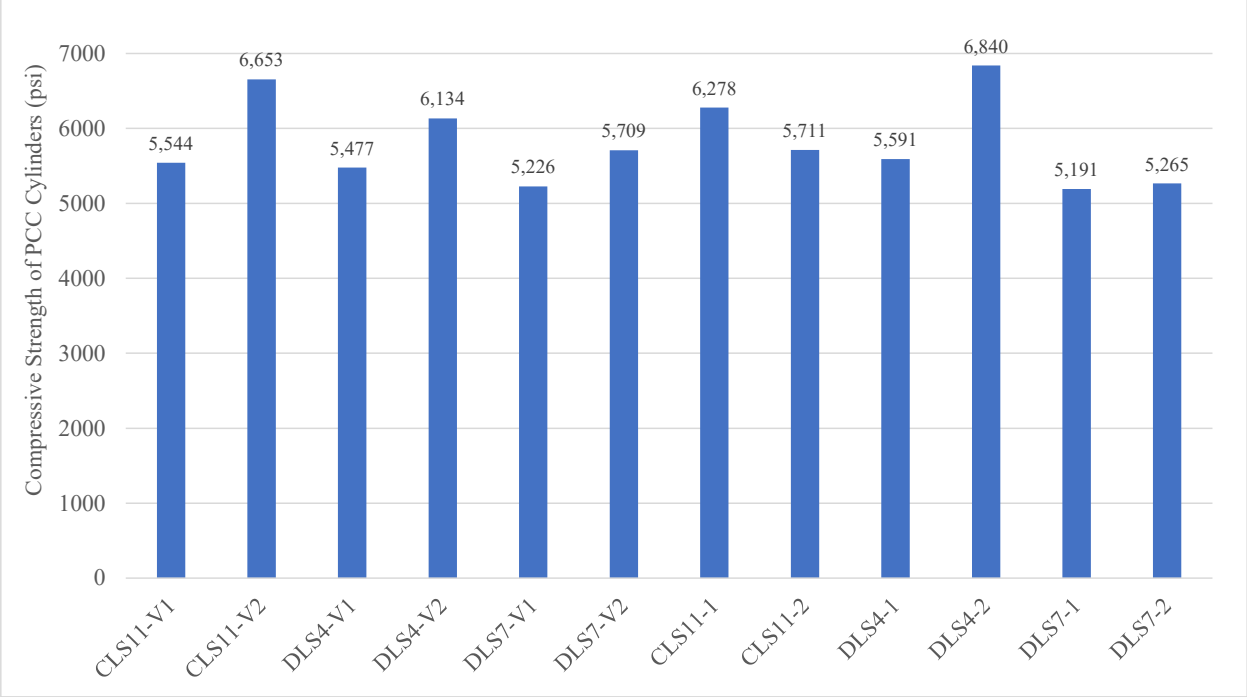

Figure 4.20: Measured compressive strength of PCC cylinders

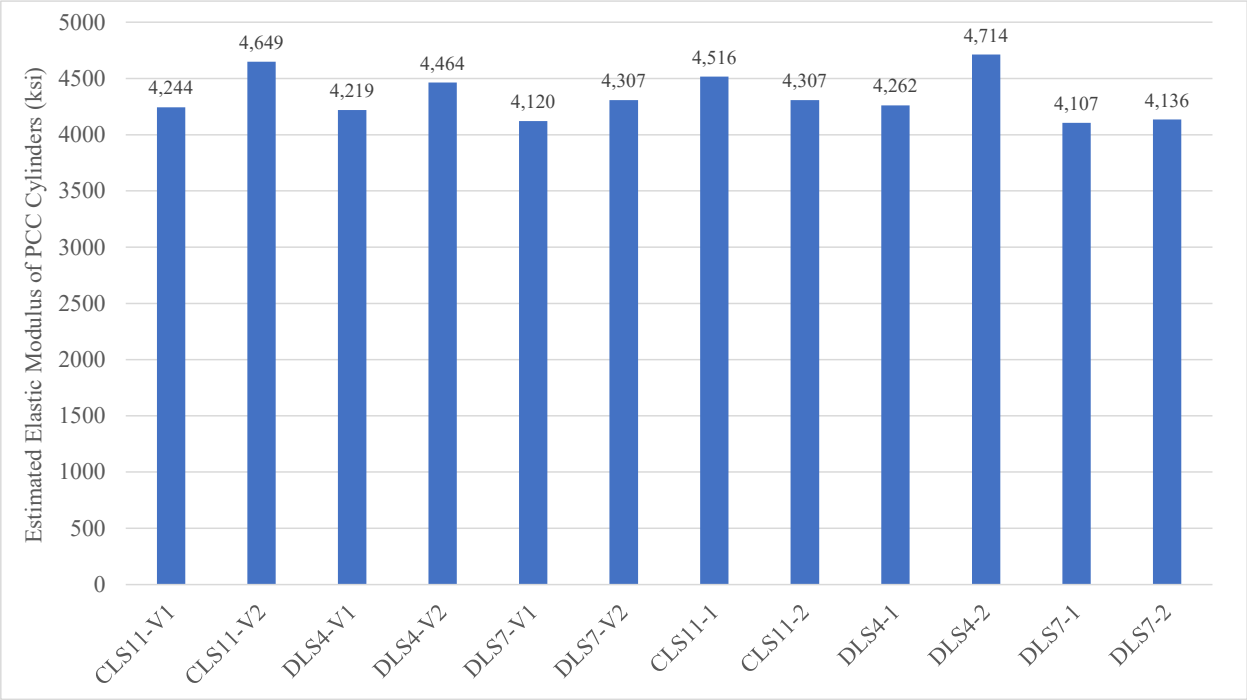

Figure 4.21: Estimated modulus of elasticity of PCC cylinders

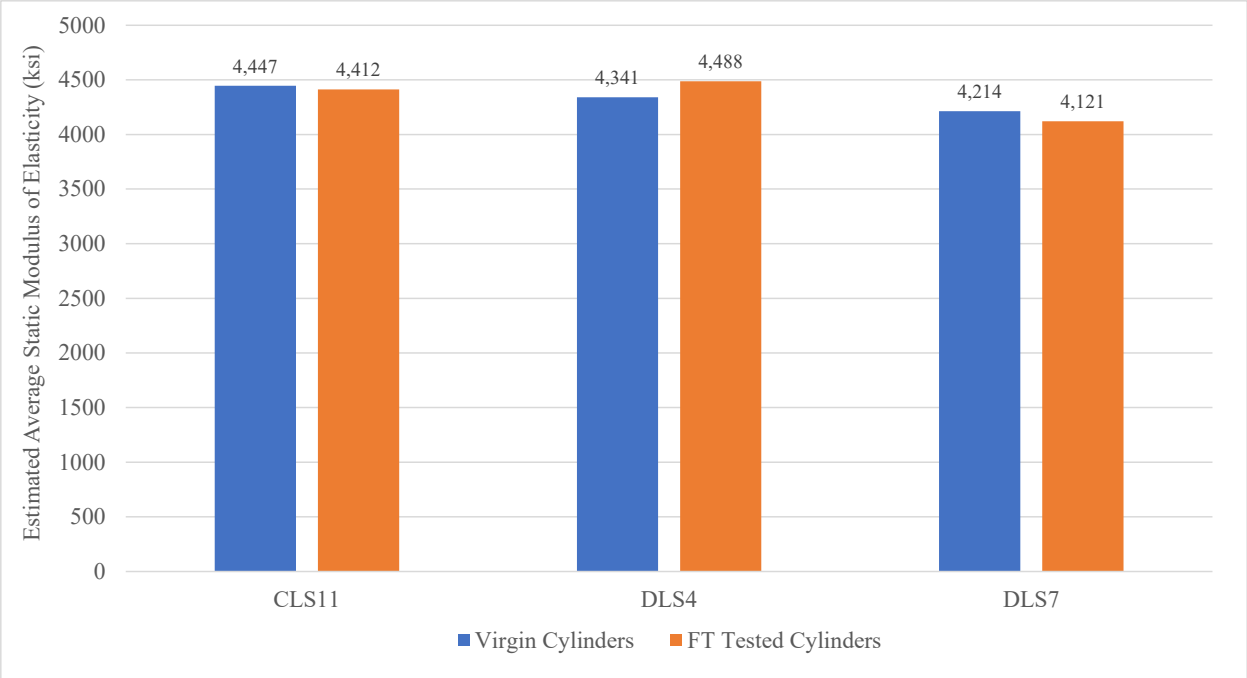

Figure 4.22: Average estimated modulus of elasticity of PCC cylinders

The estimated elastic modulus values, shown in Figure 4.21, had a maximum estimated elastic modulus of 4,714 ksi and minimum elastic modulus of 4,107 ksi. In addition, observation of the average estimated modulus values, shown in Figure 4.22, indicates that the estimated average modulus values of the freeze-thaw tested PCC cylinders were smaller than the elastic modulus values for the control specimens for PCC cylinders CLS11 and DLS7. The average estimated elastic modulus for the freeze-thaw tested PCC cylinder DLS4 was larger than the average estimated elastic modulus for the matching DLS4 control samples.

Chapter 5

Summary and Conclusions

This research investigated the durability of quarried calcareous and dolomitic limestone coarse aggregates used in PCC and in unbound base/subbase layers in Wisconsin pavements. Coarse aggregate samples were collected from various quarries in Wisconsin and were subjected to laboratory tests including the sodium sulfate soundness, freeze-thaw, and aggregate absorption tests. Furthermore, these coarse aggregates were used to prepare PCC cylinders for further testing and evaluation of strength and stiffness due to rapid freeze-thaw conditioning.

The results of the sodium sulfate soundness, freeze-thaw, and absorption tests were compared with specifications threshold limits to draw conclusions about how the collected samples compare with the WisDOT aggregate testing dataset and recommended threshold limits. The results of those tests demonstrated the following conclusions:

1) The sodium sulfate soundness test results showed that eight of the thirteen calcareous and five of the eight dolomitic limestone coarse aggregates exceeded the WisDOT threshold limit of 12%.
2) The freeze-thaw test results showed that three of the thirteen calcareous and five of the eight dolomitic limestone coarse aggregates exceeded the threshold limit of 16.8%, which corresponds to 93% passing for large set of tested Wisconsin aggregates.
3) The absorption test results showed that the calcareous and dolomitic limestone absorption values fit into the split distributions of the bimodal dataset of Wisconsin aggregate absorption values: the absorption data of the investigated 13 calcareous coarse aggregate

samples fell within the relatively high absorption distribution with an average absorption value of 2.64% and the eight dolomitic coarse aggregate samples fell within the relatively low absorption distribution with an average absorption value of 1.13%.

4) The vacuum absorption values of the investigated coarse aggregate specimens were found to be consistently larger than the standard absorption values.
5) The mass loss by sodium sulfate soundness did not have strong correlations with either absorption or the mass loss of freeze-thaw. Even though the relationship between the mass loss by sodium sulfate soundness possessed a relatively high coefficient of determination (R^2=0.86) the data had a relatively large scatter. Also, based on the limited size of dataset for this study and considering the studied aggregates were all relatively marginal in terms of freeze-thaw performance, the relationship found was not considered representative of the broader set of Wisconsin limestone coarse aggregates.
6) The presence of non-formation materials in the samples influenced the test results. Particles such as shale, chalk, chert, and other non-formation materials showed signs of significant degradation and disintegration though sodium sulfate soundness and freeze-testing.
7) No clear relationship between the chest freezer and automated freeze-thaw machine testing methods was observed. However, higher variability of testing was noted during the chest freezer testing. Freezing rates and time were inconsistent, the temperature varied at different locations in the chest freezer, and mechanical disturbance of the sample occurred during removal and replacement of the specimens during the thawing cycles. These factors may have affected the results of the chest freezer freeze-thaw test, compared with the automated freeze-thaw machine, which avoids these variability issues.

8) The compressive strength between the freeze-thaw tested and control cylinders did not significantly vary. Due to the relatively high-strength nature of the concrete mixture, it may be concluded that the high strength concrete mixture performs well when subjected to 300 rapid freeze-thaw cycles, for the tested PCC cylinders.
9) The relative dynamic modulus values of the PCC cylinders generally remained above 0.9, except for the DLS4 PCC cylinder, where the relative longitudinal and transverse E_d values dropped after 180 and 210 rapid freeze-thaw cycles, respectively. The results indicate that the PCC cylinders tested performed relatively well to the 300 rapid freeze-thaw cycle.
10) In general, the concrete mixture design used for Wisconsin pavements produced a very high-quality concrete that performed relatively well in the rapid freeze-thaw test conditioning.

References

Alexander, M., & Mindess, S. (2005). *Aggregates in concrete*. Taylor & Francis.

American Association of State Highway and Transportation Officials (AASHTO). (2021). *Standard specifications for transportation materials and methods of sampling and testing*.

American Concrete Institute (ACI). (2014). *Building code requirements for structural concrete and commentary (ACI 318R-14)*.

ASTM International. (2021). *Annual book of ASTM standards* (Vol. 04.02: Concrete and Aggregates).

Bektas, F., Cai, W., & Wang, K. (2016). (rep.). *Aggregate freezing-thawing performance using the Iowa Pore Index* (pp. 1–20). Washington, DC: U.S. Department of Transportation.

Candelaria, M. D., Kee, S.-H., Yee, J.-J., & Lee, J.-W. (2020). Effects of saturation levels on the ultrasonic pulse velocities and mechanical properties of concrete. *Materials*, *14*(1), 1–23. https://doi.org/10.3390/ma14010152

Chen, F., & Qiao, P. (2014). Probabilistic damage modeling and service-life prediction of concrete under freeze–thaw action. *Materials and Structures*, *48*(8), 2697–2711. https://doi.org/10.1617/s11527-014-0347-y

Crovetti, J. A., & Kevern, J. T. (2018). (rep.). *Joint sawing practices and effects on durability* (pp. 1–152). Madison, WI: Wisconsin Department of Transportation WHRP.

Dashti, D. (2016). *A study of the NDT techniques using ultrasonic pulse velocity test and microwave oven method on Scc and Tvc* (thesis). West Virginia University, Morgantown.

Hamoush. (2011). Freezing and thawing durability of very high strength concrete. *American Journal of Engineering and Applied Sciences*, *4*(1), 42–51. https://doi.org/10.3844/ajeassp.2011.42.51

IAEA. (2002). (rep.). *Guidebook on non-destructive testing of concrete structures* (pp. 1–205). Vienna, Austria: International Atomic Energy Agency.

Koubaa, A., Snyder, M. B., & Peterson, K. R. (1997). (rep.). *Mitigating concrete aggregate problems in Minnesota* (pp. 1–201). St. Paul, MN: Minnesota Department of Transportation.

Laberge, G. L. (1984). The geologic history of Wisconsin. *Rocks & Minerals*, *59*(2), 61–73. https://doi.org/10.1080/00357529.1984.11764448

McLeod, H. A. K., Welge, J., & Henthorne, R. (2014). (rep.). *Aggregate freeze-thaw testing and D-cracking field performance: 30 years later* (pp. 1–31). Topeka, KS: Kansas Department of Transportation Bureau of Research.

Michigan Department of Trasnportation. (2022). (publication). *Manual for the Michigan test methods (MTM)*. MDOT.

Minnesota Department of Transportation. (2020). MnDOT Standard Specifications for Construction. Retrieved June 20, 2022, from dot.state.mn.us/pre-letting/spec/

Myers, J. D., & Dubberke, W. (1980). (rep.). *Iowa Pore Index Test* (pp. 1–4). IDOT Highway Division Office of Materials.

Obla, K. H., Kim, H., & Lobo, C. L. (2016). Criteria for freeze-thaw resistant concrete mixtures. *Advances in Civil Engineering Materials*, *5*(2), 20150005. https://doi.org/10.1520/acem20150005

Pigeon, M., & Pleau, R. (1995). *Durability of concrete in cold climates*. E. & F.N. Spon.

Powers, T. C. (1945). A working hypothesis for further studies of Frost resistance of concrete. *ACI Journal Proceedings*, *41*(4), 245–272. https://doi.org/10.14359/8684

Qiao, P., McLean, D. I., & Chen, F. (2012). (rep.). *Concrete performance using low-degradation aggregates* (pp. 1–90). Olympia, WA: Washington State Department of Transportation Office of Research & Library Services.

Richardson, D. N. (2009). (rep.). *Quick test for durability factor estimation* (pp. 1–99). Rolla, MO: Missouri Department of Transportation Research, Development and Technology.

Sherrill, M. G. (1978). (publication). *Geology and ground water in Door County, Wisconsin, with emphasis on contamination potential in the Silurian Dolomite* (Ser. Geological Survey Water-Supply Paper, pp. 1–38). United States Department of the Interior.

Staton, J. F., & Anderson, J. D. (2009). (rep.). *Absorption capacity of coarse aggregates for Portland cement concrete* (pp. 1–50). Lansing, MI: Michigan Department of Transportation.

Tabatabai, H., Titi, H., Lee, C.-W., Qamhia, I., & Puerta Fella, G. (2013). (rep.). *Investigation of testing methods to determine long-term durability of Wisconsin aggregates* (pp. 1–90). Madison, WI: Wisconsin Department of Transportation WHRP.

Titi, H., El-Hajjar, R., and Tabatabai, H. (2022). “Wisconsin Aggregate Quality,” Final Report, Wisconsin Highway Research Program, Madison, WI, 50 p.

Trifone, L. (2017). A study of the correlation between static and dynamic modulus of elasticity on different concrete mixes. *Graduate Theses, Dissertations, and Problem Reports*. https://doi.org/10.33915/etd.6833

Weyers, R. E., Williamson, G. S., Mokarem, D. W., Lane, D. S., & Cady, P. D. (2005). (rep.). *Testing methods to determine long term durability of Wisconsin aggregate resources* (pp. 1–69). Madison, WI: Wisconsin Department of Transportation WHRP.

Williams, S. G., & Cunningham, J. B. (2012). (rep.). *Evaluation of aggregate durability performance test procedures* (pp. 1–74). ArDOT Transportation Research Committee.

Wisconsin Department of Transportation. (2017, March 31). Wisconsin Department of Transportation Geotechnical Manual. Retrieved June 5, 2022, from https://wisconsindot.gov/Pages/doing-bus/eng-consultants/cnslt-rsrces/geotechmanual/default.aspx

Wisconsin Department of Transportation. (2022, May 17). Wisconsin Department of Transportation Facilities Development Manual (FDM). Retrieved June 1, 2022, from https://wisconsindot.gov/pages/doing-bus/eng-consultants/cnslt-rsrces/rdwy/fdm.aspx

Wisconsin Geological and Natural History Survey. (2005). Bedrock Geology of Wisconsin. map, Madison, Wisconsin.